THE ASTROPHYSICAL JOURNAL SUPPLEMENT SERIES, 59:161–181, 1985 October

HIGH SIGNAL-TO-NOISE RATIO OBSERVATIONS OF H I IN 243 GALAXIES

B. M. LEWIS
Arecibo Observatory, National Astronomy and Ionosphere Center
G. HELOU
Infrared Processing and Analysis Center, California Institute of Technology
AND
E. E. SALPETER
Center for Radiophysics and Space Research, Cornell University
Received 1985 February 15; accepted 1985 April 19

ABSTRACT

We used the 21 cm spectral-line system of the Arecibo Observatory to measure neutral hydrogen emission from 243 faint galaxies. Most lie near the plane of the Local Supercluster. All observations reach an unsmoothed signal-to-noise ratio of at least 7.0; the average for the set is 23. The resulting data are used to estimate H I masses, systemic velocities, and accurate profile widths at 20%, 25%, 50%, and 80% of peak intensity levels. We use the widths to calibrate directly the bias introduced by popular data-smoothing operations. Our data include observations of 65 objects with previously unknown redshifts.

Subject headings: galaxies: redshifts — line profiles — radio sources: galaxies — radio sources: 21 cm radiation

I. INTRODUCTION

The physical reality of "superclusters" of galaxies is well established. Extensive redshift surveys of galaxies such as the Center for Astrophysics Survey of Huchra *et al.*, (1983, hereafter CfA) confirm the isolation in redshift distributions between adjacent superclusters found by Gregory and Tifft (1976) in the direction of Coma, and substantiate the existence of voids in the general distribution of galaxies (cf. Gregory and Thompson, 1978; Davis *et al.* 1982). Superclusters often appear to be extended sheetlike structures, containing one or several dense clusters of galaxies. These are sometimes quasi-spherical (Coma), sometimes predominantly filamentary or cigar-shaped structures (Perseus), and sometimes planar (Virgo). Recent increases in available redshifts emphasize the filamentary substructure permeating Virgo (cf. Tammann 1983; Huchra 1983).

The detailed study of superclusters is just beginning. While fairly extensive surveys exist for the neighboring Abell 1327/Coma, Hercules, and Perseus-Pisces superclusters, detailed work on our local Virgo supercluster has been slower. This is due in part to the number of objects that need to be surveyed and in part to the larger errors incurred in using redshift distances, which are affected by peculiar velocities relative to Virgo of both the Local Group and the objects themselves. Many of the initial studies were completed by de Vaucouleurs in a series of papers leading up to his 1976 work; recent papers by Tully (1982) and by Aaronson *et al.* (1982) rely heavily on the M_B–velocity width relation found by Tully and Fisher (1977) to remove distance ambiguities.

We wish to explore the relationship between the Virgo Cluster and its surrounding supercluster, and so are observing H I profiles for the fainter galaxies in the *Uppsala General Catalogue* (Nilson 1973, hereafter UGC), which are in the plane of the Local Supercluster. We pay particular attention to the accuracy of H I profile widths, so distances can be estimated from the Tully-Fisher relation. Results from the first year of this study are presented here for objects with an unsmoothed signal-to-noise ratio in excess of 7. These include observations of 65 galaxies with previously unknown redshifts.

II. OBSERVATIONS

Our sources are fainter than $m \sim 12.0$, are from the UGC, and lie in the 9^h–16^h zone about the plane of the Local Supercluster as it is accessible from Arecibo. The Virgo and Coma cluster regions are excluded, as are galaxies with a spheroidal or elliptical classification. Objects with axis ratios $b/a > 0.867$ are covered by Lewis (1985*a*) in a companion paper. We chose to observe first those objects brighter than 14.6 mag with known velocities, then to work progressively through the list to successively smaller angular diameter limits. Our results reflect both these priorities and a concentration of observing time on objects with velocities below ~ 6000 km s^{-1}.

The observations were made with the Arecibo 305 m telescope during 1983, using a cooled GaAs field effect transistor amplifier, which gives a system temperature of about 40 K near the zenith. The receiver is fed by a 12 m long dual-polarization line feed, which illuminates an annulus with an outside diameter of 213 m and a hole of diameter 91 m to yield a FWHP beam of $\sim 3'.3$. The signal is fed to a one-bit 1008 channel autocorrelator split into four 10 MHz quads. These are used to observe two copies of each polarization when the systemic velocity is known, or to search a 30 MHz wide section of the spectrum at one time. The resulting channel spacing is ~ 8.2 km s^{-1}. Fluxes are calibrated using small angular diameter sources listed in Bridle *et al.* (1972).

Most sources were observed in the total power mode, with 5 minutes ON source followed by 5 minutes OFF. The OFF is positioned to track exactly the same range of azimuth and elevation as the ON, to ensure flat stable baselines. Source positions are taken from Dressel and Condon (1976), or are refined by generating overlays for the Palomar Observatory Sky Survey prints, to yield positions with an accuracy of $\sim 6''$.

We want accurate widths from the H I profiles to estimate distances using the Tully-Fisher relation. The prerequisite for this is an adequate signal-to-noise ratio. When this is defined as the ratio between the peak "horn" intensity and the rms noise in the baseline, Lewis (1983*a*) finds that a signal-to-noise ratio of 7.0 is usually sufficient to obtain 20% widths with a confidence interval smaller than ± 10 km s^{-1}. Figure 1 shows our observations of the central positions of galaxies for which we have obtained unsmoothed profiles with a signal-to-noise ratio of at least 7.0. Most objects were observed several times to obtain this signal-to-noise level. Since the Arecibo telescope has a significant zenith-angle–dependent gain variation, our observations are calibrated before removing a simple polynomial baseline and interference spikes. The processed spectra are then combined with a weight in inverse proportion to the square of the rms deviations about the baseline. Final spectra after a single "von Hann convolution" are shown in Figure 1.

III. RESULTS

All widths are evaluated using impersonal algorithms that follow the precepts of Lewis (1983*a*). Their efficacy is checked by comparing smoothed and unsmoothed 50% widths, which showed that 6% of the sample has differences ≥ 15 km s^{-1}. These cases were reduced again individually and are recorded in column (12) of Table 1 with an asterisk. Generally the interior region between the "horns" of the profile needed adjustment, so widths could be estimated with the usual algorithms. A second check is to plot a differential width diagram between the 20% and 80% widths and the 20% and 50% widths, and then ensure that the widths of outliers are reliable. Figure 2 shows the final form of this diagram.

Automatic algorithms deal effectively with "two-horned" and single-peaked profiles; misleading results arise when profiles are composites of several components (e.g., UGC 5561, UGC 9595, UGC 9794, and UGC 10202) or are distorted (UGC 8774, UGC 9904), or when the signal-to-noise ratio is too low. The worst example is UGC 6623, which appears to be a superposition of several regular two-horned profiles and has a 50% width change from smoothed to unsmoothed of ~ 145 km s^{-1}. The differences between smoothed and unsmoothed 50% widths after any reprocessing are plotted in Figure 3 against the signal-to-noise ratio. The mean unsmoothed signal-to-noise ratio for the whole sample is ~ 23. While a few differences ≥ 10 km s^{-1} occur, most are small. The largest remaining is a difference of ~ 33 km s^{-1} due to UGC 8774 with a signal-to-noise ratio of 7.1. Figure 4 shows histograms of the differences between smoothed and unsmoothed 10%, 20%, 25%, 50%, and 80% widths and the systemic velocity estimates. In general, smoothing an H I profile rounds the intensity of the horn down and so increases the measured width. The histograms exhibit the expected bias toward overestimating widths, which increases steadily as the percentage level drops and increases as the degree of smoothing increases.

Table 2 lists the bias and its dispersion about the mean in comparisons on our data set between unsmoothed values, on the one hand, and both "Hanned" (Hanning smoothed) and "Hanned" with boxcar smoothing over three channels used by both Giovanardi and Salpeter (1985, hereafter GS) and Haynes and Giovanelli (1984). While the 80% level has the smallest bias, its variance is similar to that at the 10% level. At the much-used 20% level, smoothing increases the width estimates on average by 3.1 ($\sigma \approx 1.9$) km s^{-1}, while the alternate smoothing scheme increases them by 7.3 ($\sigma \approx 3.4$) km s^{-1}. Table 2 shows that successive smoothing operations increase both the bias and the variance almost linearly. Operationally the 50% and 25% widths are the most reliable estimators of profile width and should be the levels adopted by choice.

To preserve precision, unsmoothed widths are recorded in Table 1, except for a few estimates with large initial differences between smoothed and unsmoothed parameters. These are replaced with "Hanned" widths reduced by the appropriate bias noted in Table 2. Table 1 lists the H I parameters for galaxies in our sample, together with those of a few other objects observed as time permitted. For homogeneity of presentation, Table 1 also includes data on objects discussed by Lewis (1983*a*, *b*, 1985*b*). The entries are described below.

Column (1).—UGC number, preceded by an asterisk when no previous velocity is known.

Column (2).—Alternative NGC, IC, or DDO label.

Columns (3) and (4).—Observed right ascension ($xx^h xx^m xx^s$) and declination ($xx°xx'xx''$) at epoch 1950.0.

Columns (5) and (6).—UGC type and blue axis sizes.

Column (7).—Zwicky magnitude listed in UGC.

Column (8).—Heliocentric systemic velocity in km s^{-1}, evaluated from the midpoint of the "Hanned" 50% profile width in the optical convention $V = c\Delta\lambda/\lambda_0$.

Columns (9)–(12).—Unsmoothed width estimates in km s^{-1}; no adjustment is made for galaxy inclination, redshift, or residual smoothing.

Column (13).—Asymmetry index for the gas distribution in the two halves of the profile. Symmetrical profiles have a value of unity.

Column (14).—Area under the profile (flux integral).

Column (15).—Adjustment factor for beam dilution, following equation (7) of Hewitt, Haynes, and Giovanelli (1983).

Column (16).—Total hydrogen mass in units of 10^9 $M_\odot$ after adjustment for beam dilution; no correction is made for self-absorption. Distance estimates assume $H = 50$ km s^{-1} Mpc^{-1}.

Columns (17) and (18).—Root mean square noise in baseline, and signal-to-noise ratio.

a) Hydrogen Mass

The estimation of H I masses in galaxies using the Arecibo beam was carefully analyzed and calibrated by Hewitt, Haynes, and Giovanelli (1983). We use their equation (7) to adjust the observed flux integral for the effects of extended source size. Giving unit weight to each observation, we fit

$$\log M_{\rm H}(\rm adj) = 7.16 + 1.71 \log D_{25}\ (\rm kpc),$$

where D_{25} is the blue diameter at the 25 mag arcsec^{-2} isophote. Our observations with this fit are shown in Figure 5.

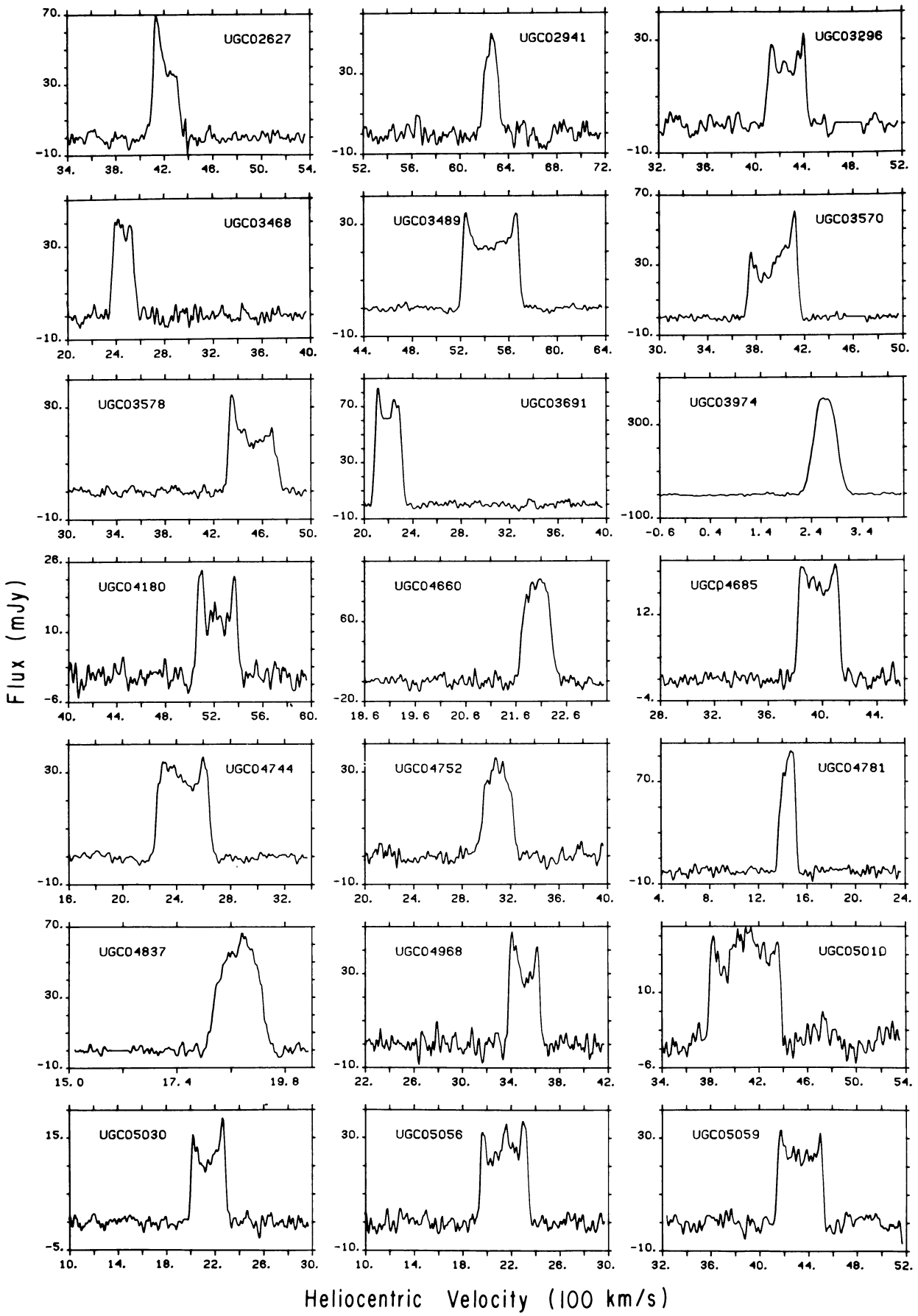

FIG. 1.—Profiles of new observations after Hanning smoothing. A polynomial baseline and occasional interference spikes have been removed.

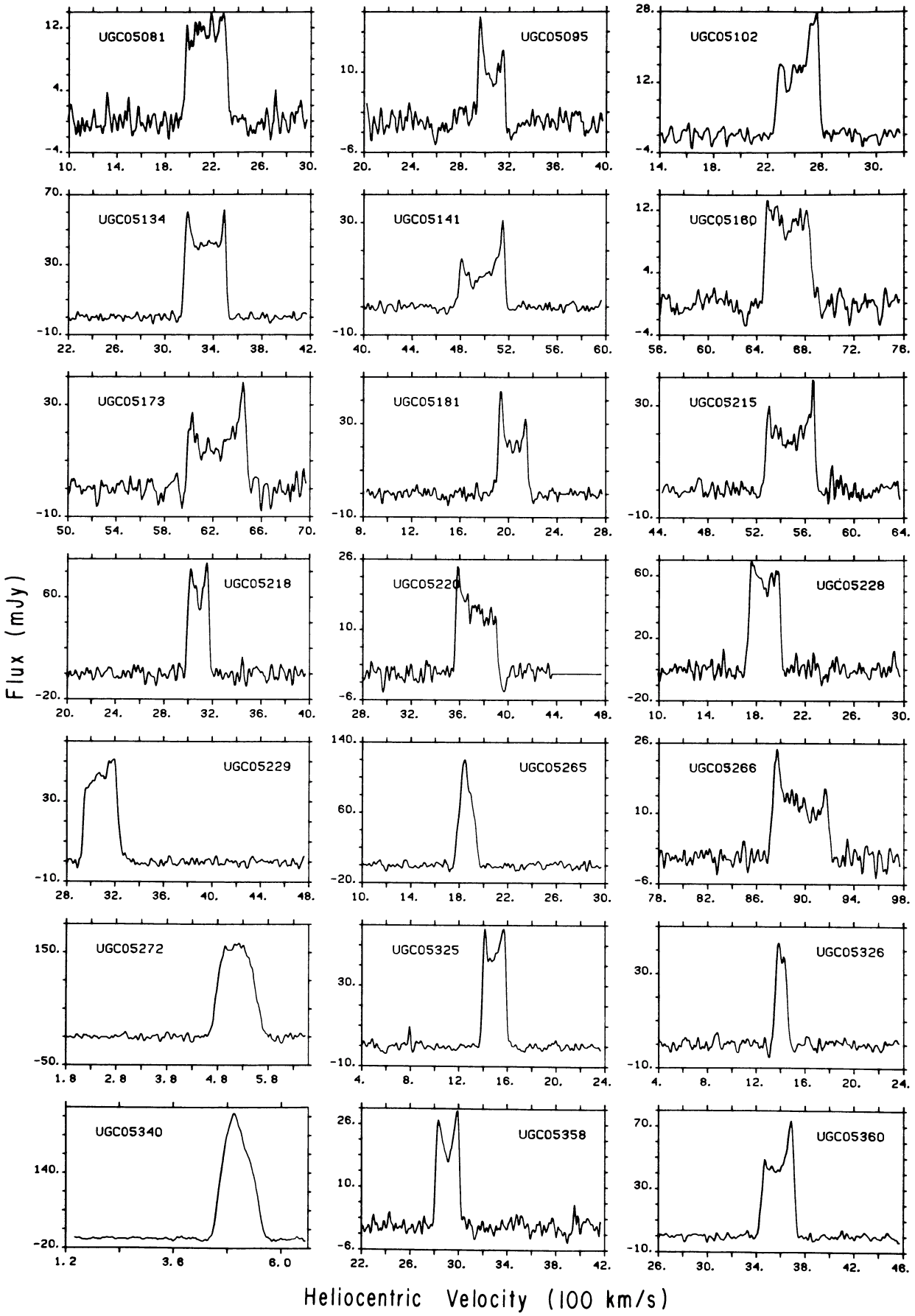

FIG. 1—*Continued*

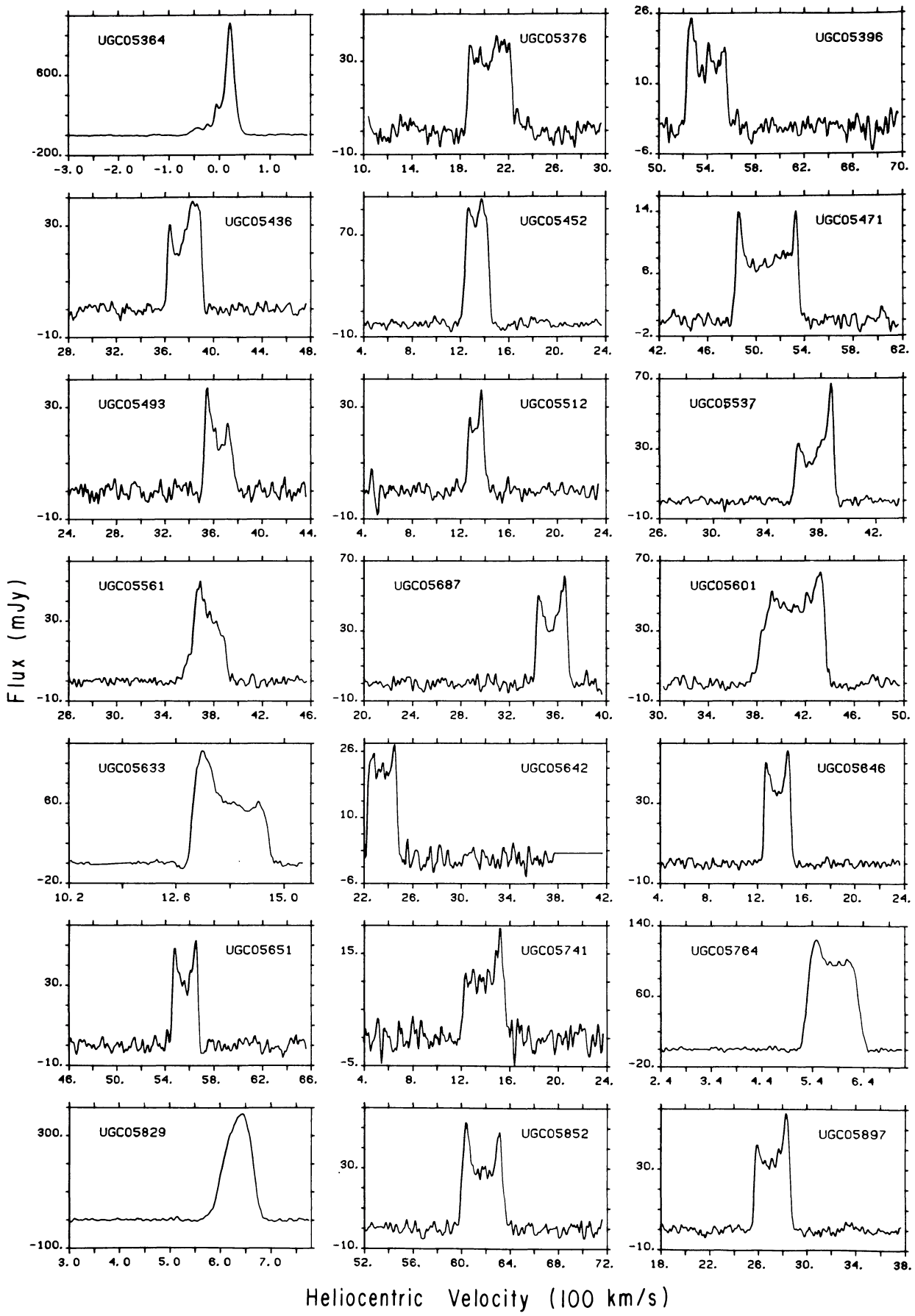

FIG. 1—*Continued*

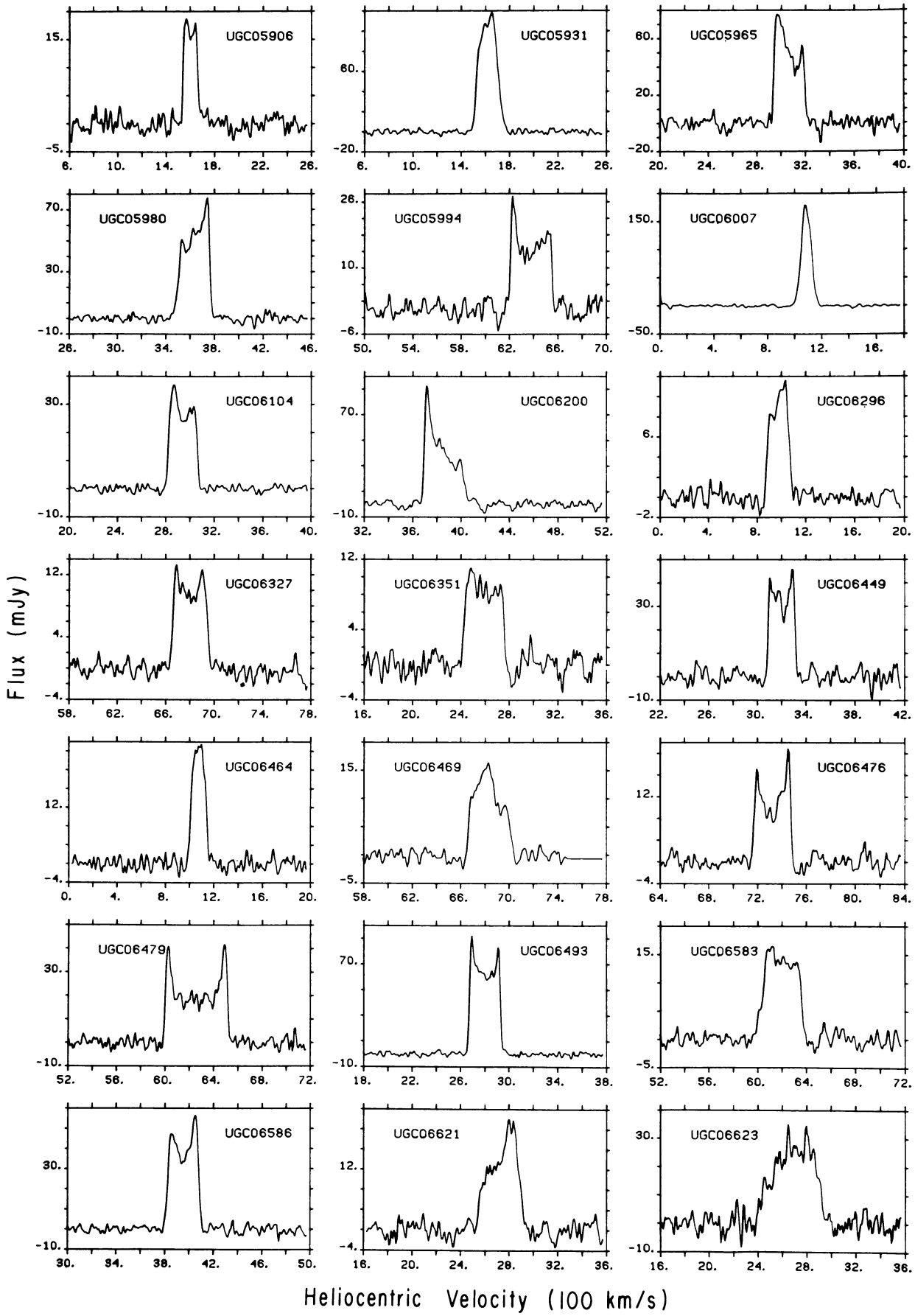

FIG. 1—*Continued*

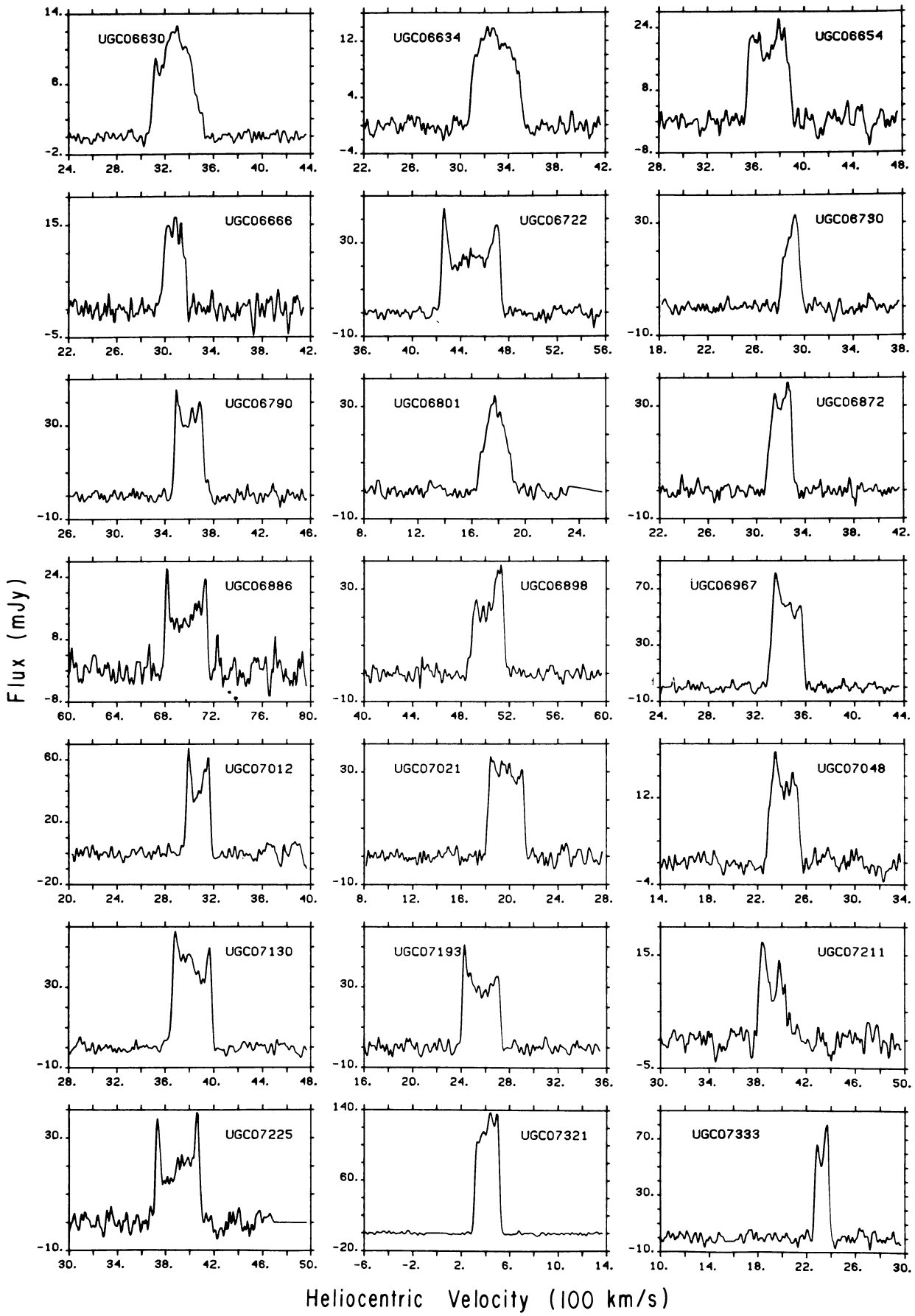

FIG. 1—*Continued*

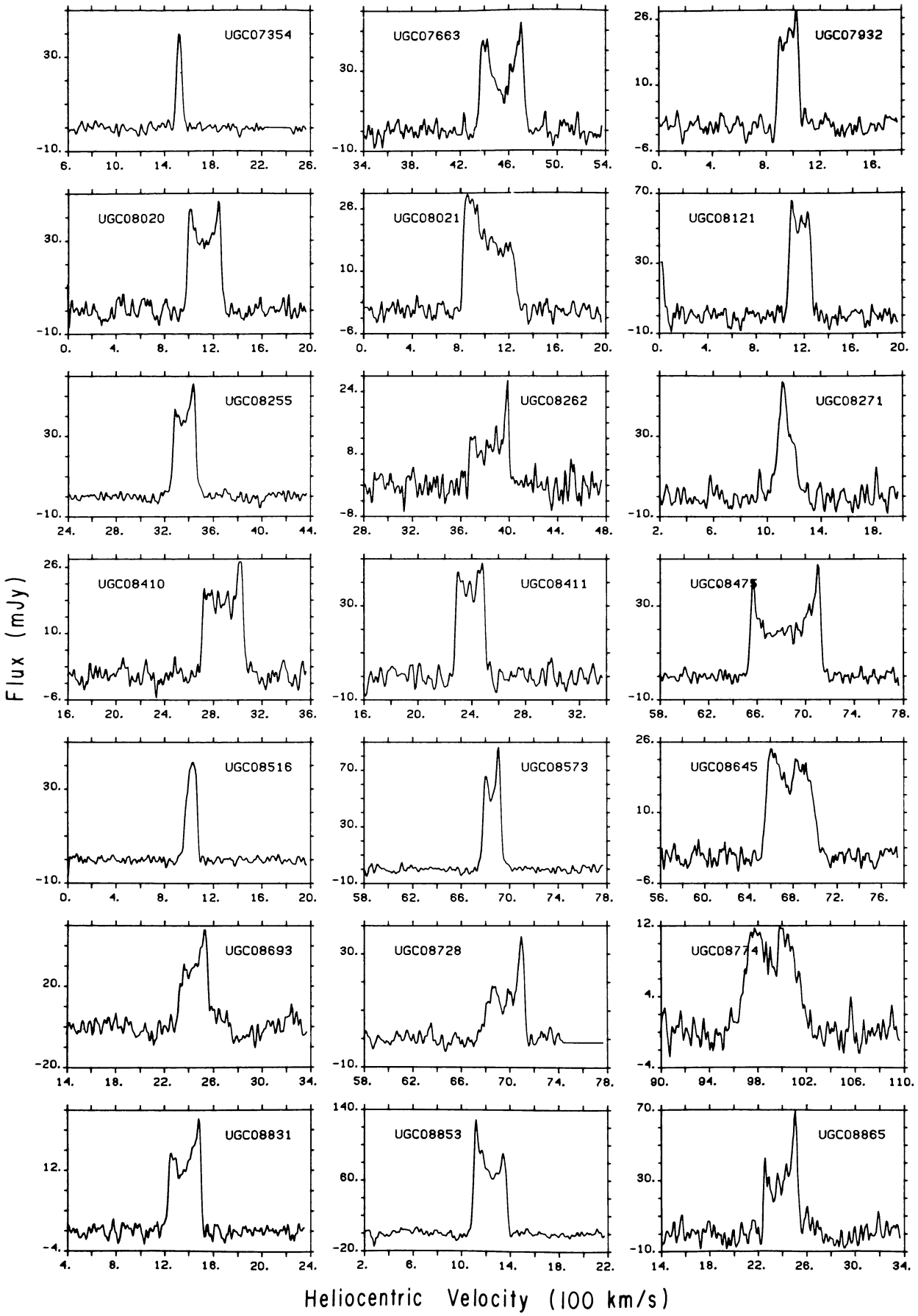

FIG. 1—*Continued*

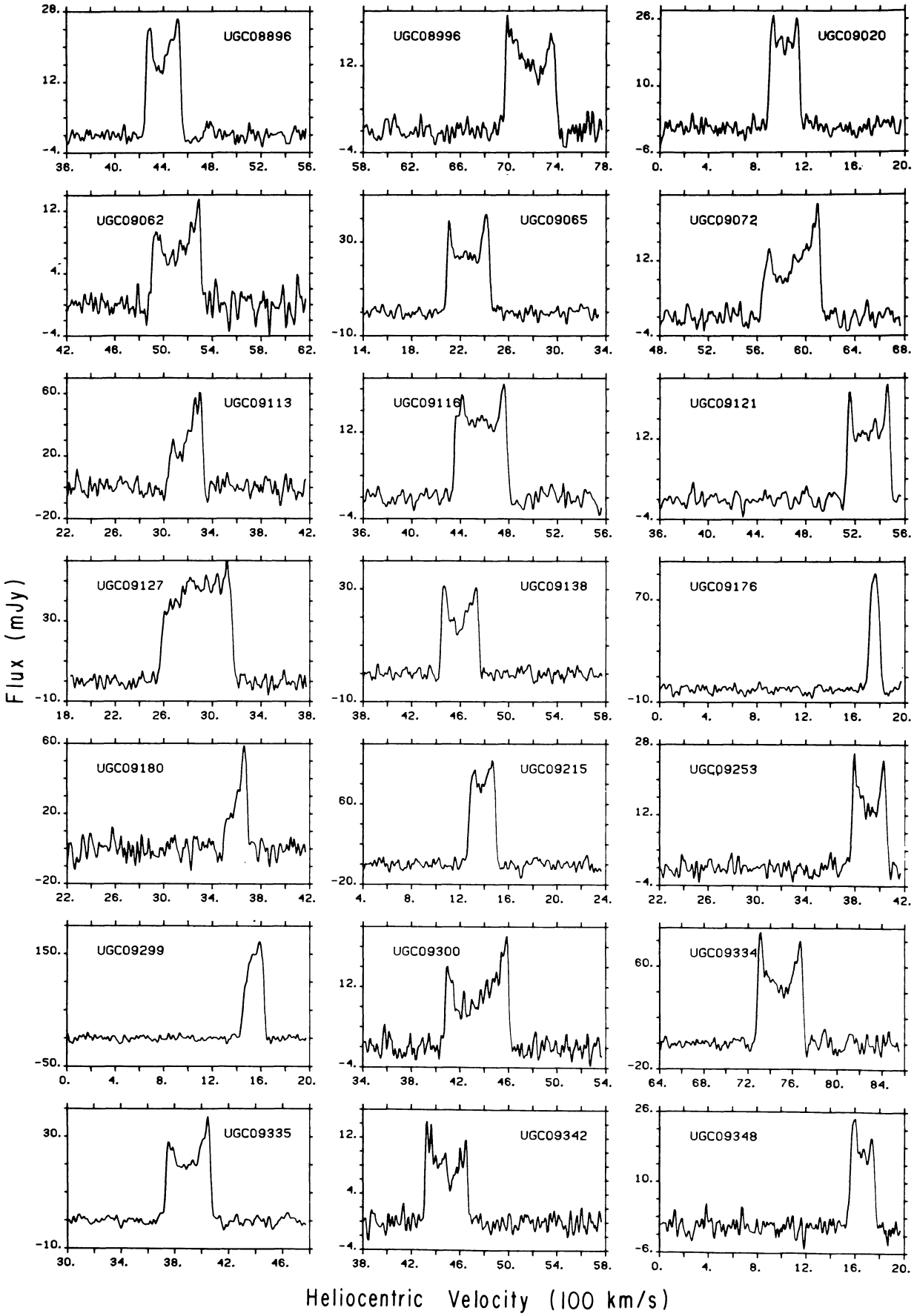

FIG. 1—*Continued*

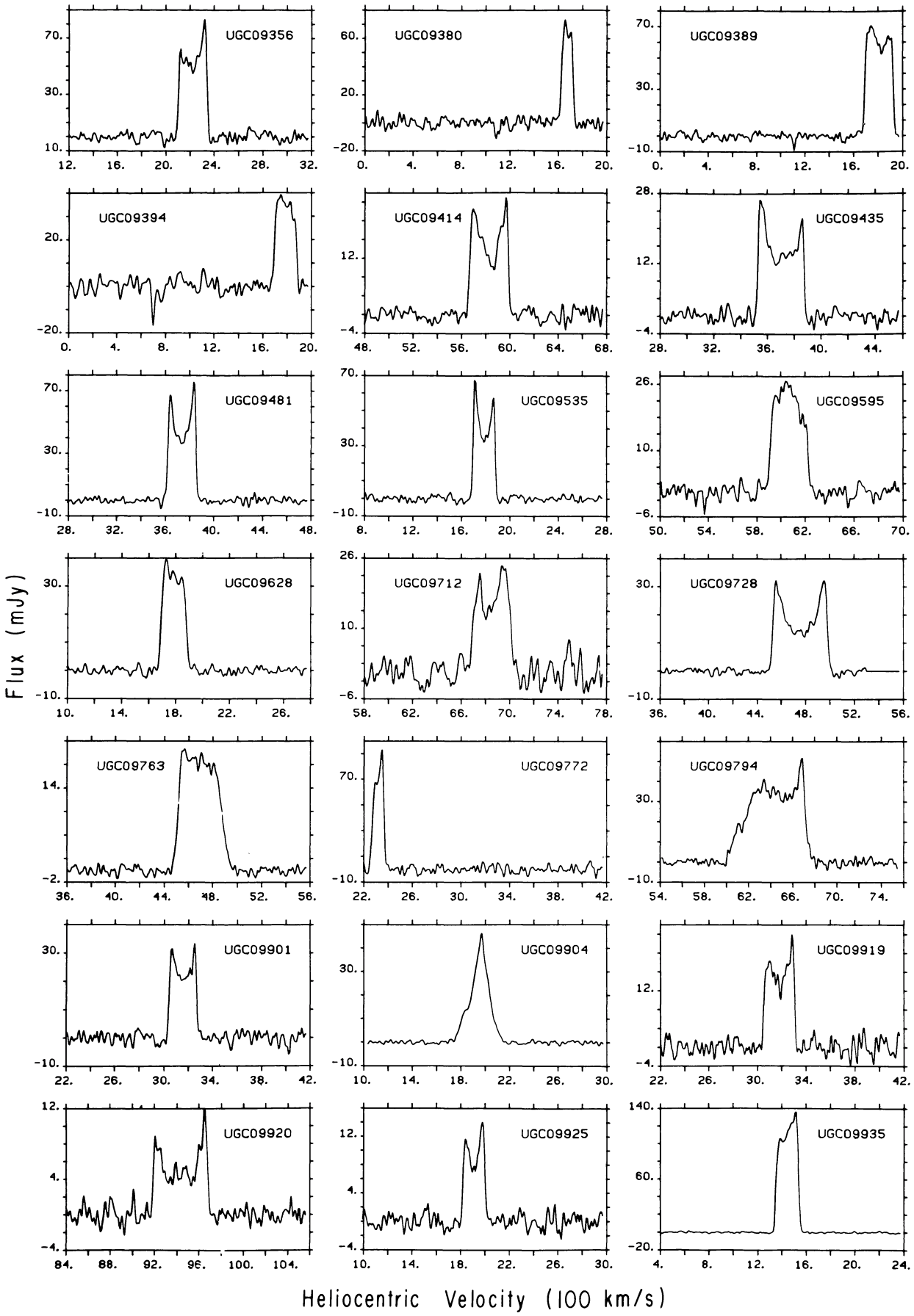

FIG. 1—*Continued*

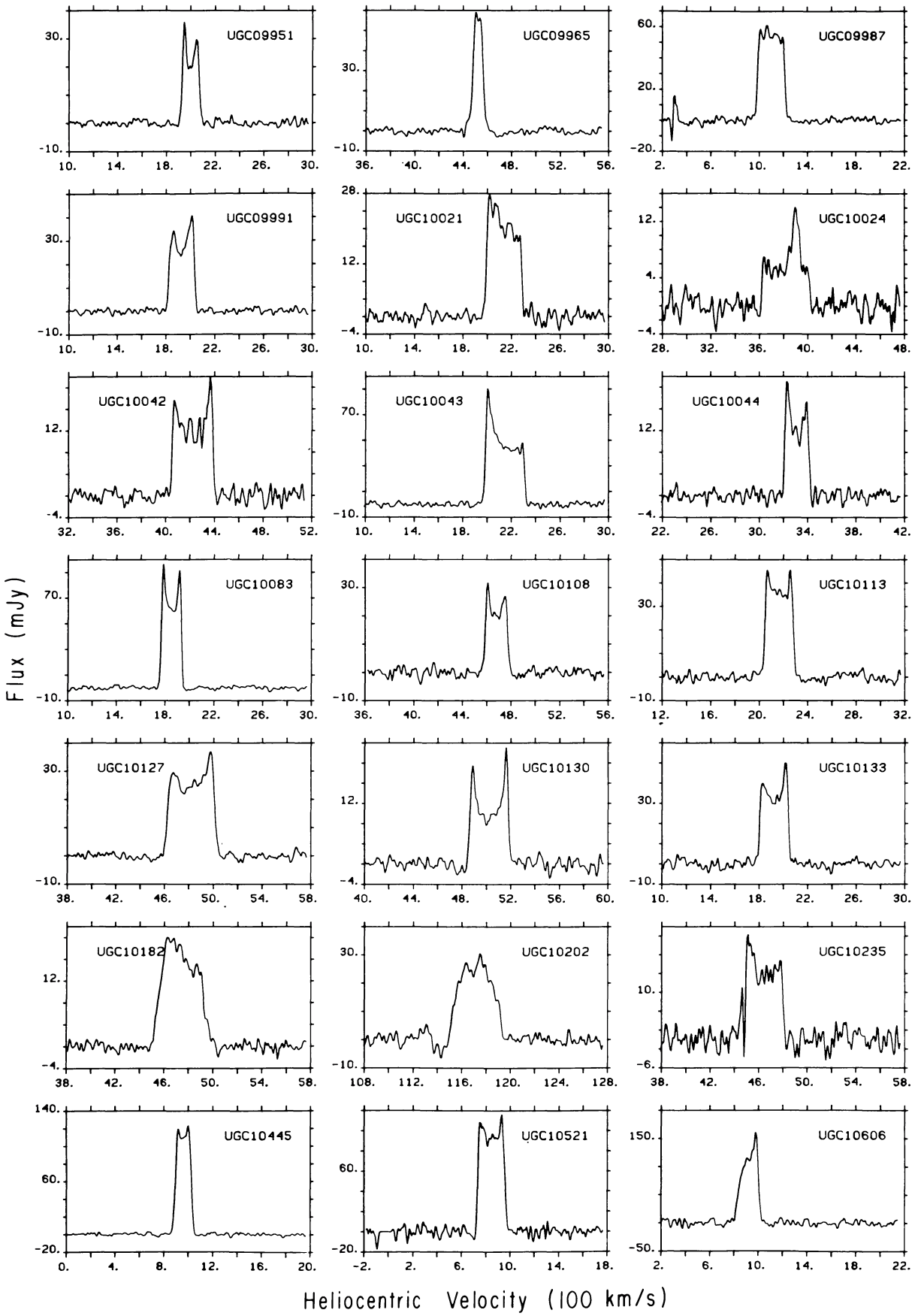

FIG. 1—*Continued*

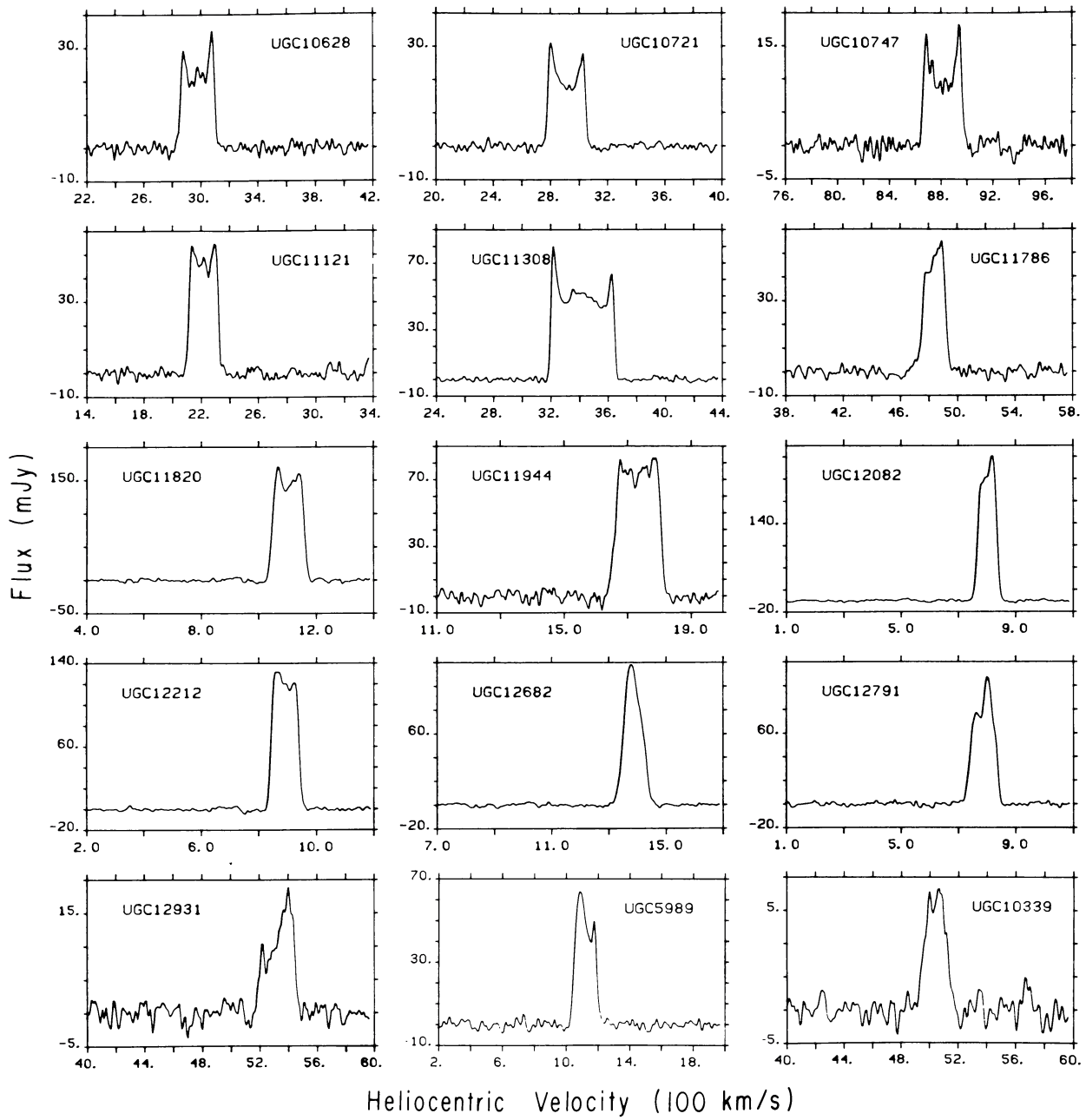

FIG. 1—*Continued*

This regression is negligibly different from that fitted to the whole isolated galaxy sample by Haynes and Giovanelli (1984), which suggests that the two samples have similar H I environments.

b) Asymmetrical Profiles

The occurrence of asymmetrical profiles may be increased by our assumption that the integral profile can be approximated by the profile obtained by pointing the telescope at the center of the galaxy, when pointing errors are a significant factor while observing objects with a size comparable to the beam. This is probably the cause of the asymmetry seen in UGC 12931 and may also be the cause of the asymmetries seen in UGC 6200, UGC 8021, and UGC 9180. We test for this as a general factor by comparing the asymmetry index S (the ratio of the areas in the two halves of the profile) for galaxies with major axes $a < 2'.0$ with the value obtained from the whole sample. Discarding three values of $S > 2.0$ for UGC 5364 (Leo A), UGC 9113, and UGC 12613 (DDO 216), we obtain

$$\langle S \rangle = 1.20\,(\sigma \approx 0.18); \qquad n = 141,$$

compared with

$$\langle S \rangle = 1.19\,(\sigma \approx 0.22); \qquad n = 240.$$

We conclude that pointing errors are unimportant here.

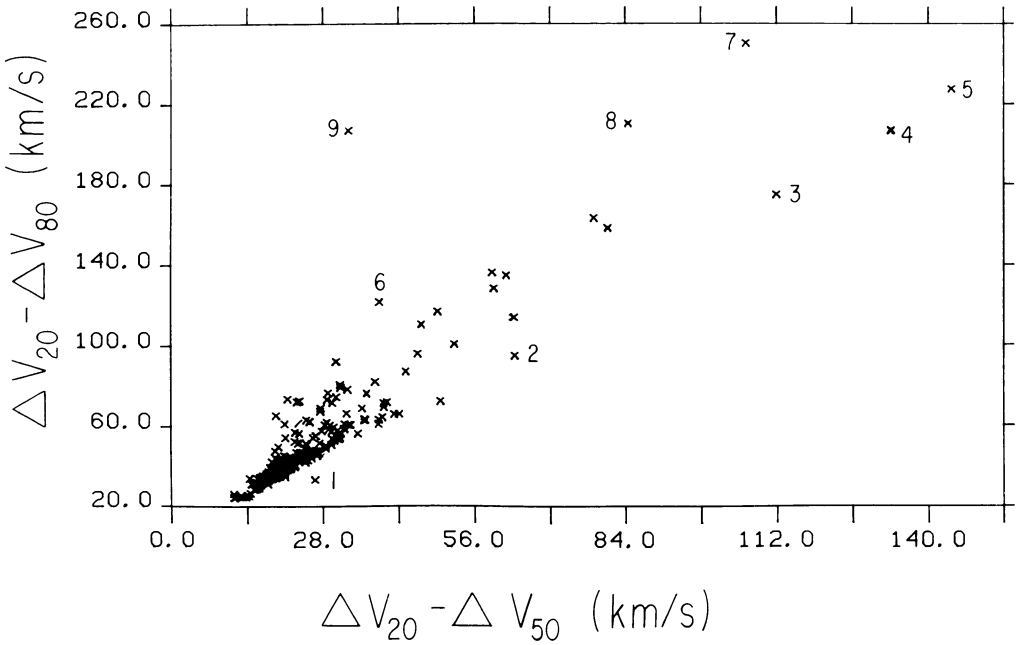

FIG. 2.—A differential width diagram, in which the difference between 20% and 80% Hanned widths is plotted against the difference between the 20% and 50% widths. Numbered outliers are as follows: 1 = UGC 5364, 2 = UGC 6583, 3 = UGC 8774, 4 = UGC 9904, 5 = UGC 9794, 6 = UGC 9595, 7 = UGC 5561, 8 = UGC 10202, and 9 = UGC 9127.

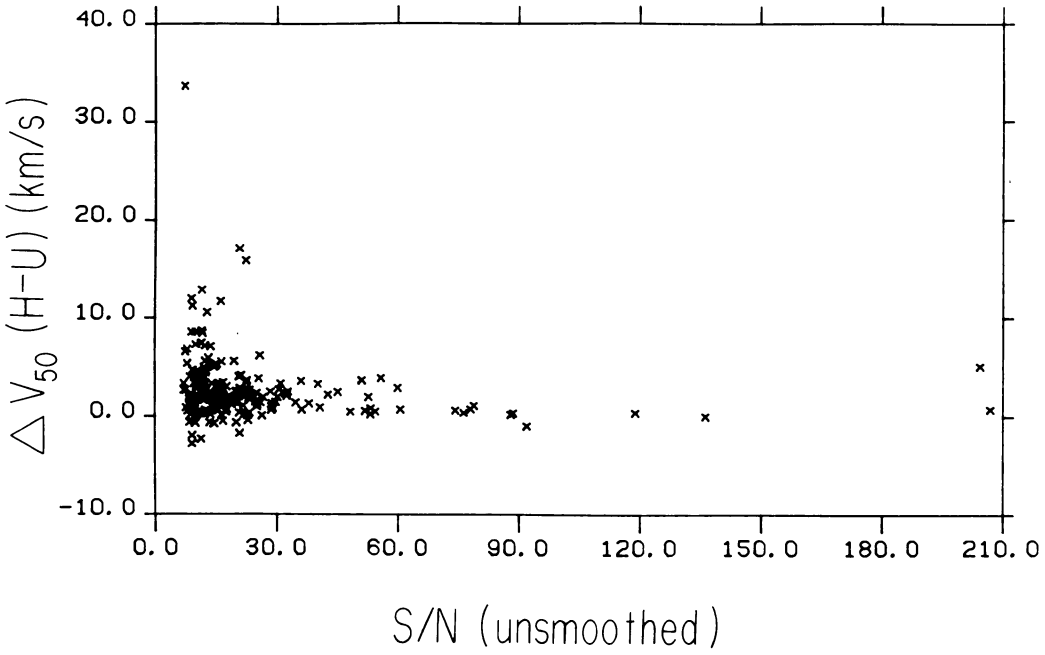

FIG. 3.—The difference between Hanned and unsmoothed 50% widths is plotted against the unsmoothed signal-to-noise ratio

c) Width Estimates

For signal-to-noise ratios exceeding 7, the expected error in a measured width is ± 5 km s^{-1} at 50% and ± 6 km s^{-1} at 20% level (cf. Lewis 1983*a*). Widths depend little on whether the central profile or a composite integral profile is measured. We therefore compare our results with those of Giovanardi and Salpeter (1985) evaluated using similar precepts.

We compare widths from our "Hanned" and 3 channel boxcar-smoothed profiles with those from GS objects having a signal-to-noise ratio larger than 10. This yields

$$\langle \Delta V - \Delta V_{GS} \rangle = 1.56\ (\sigma \approx 3.31)\ \text{km s}^{-1} \quad (50\%),$$

$$\langle \Delta V - \Delta V_{GS} \rangle = 2.98\ (\sigma \approx 6.36)\ \text{km s}^{-1} \quad (20\%).$$

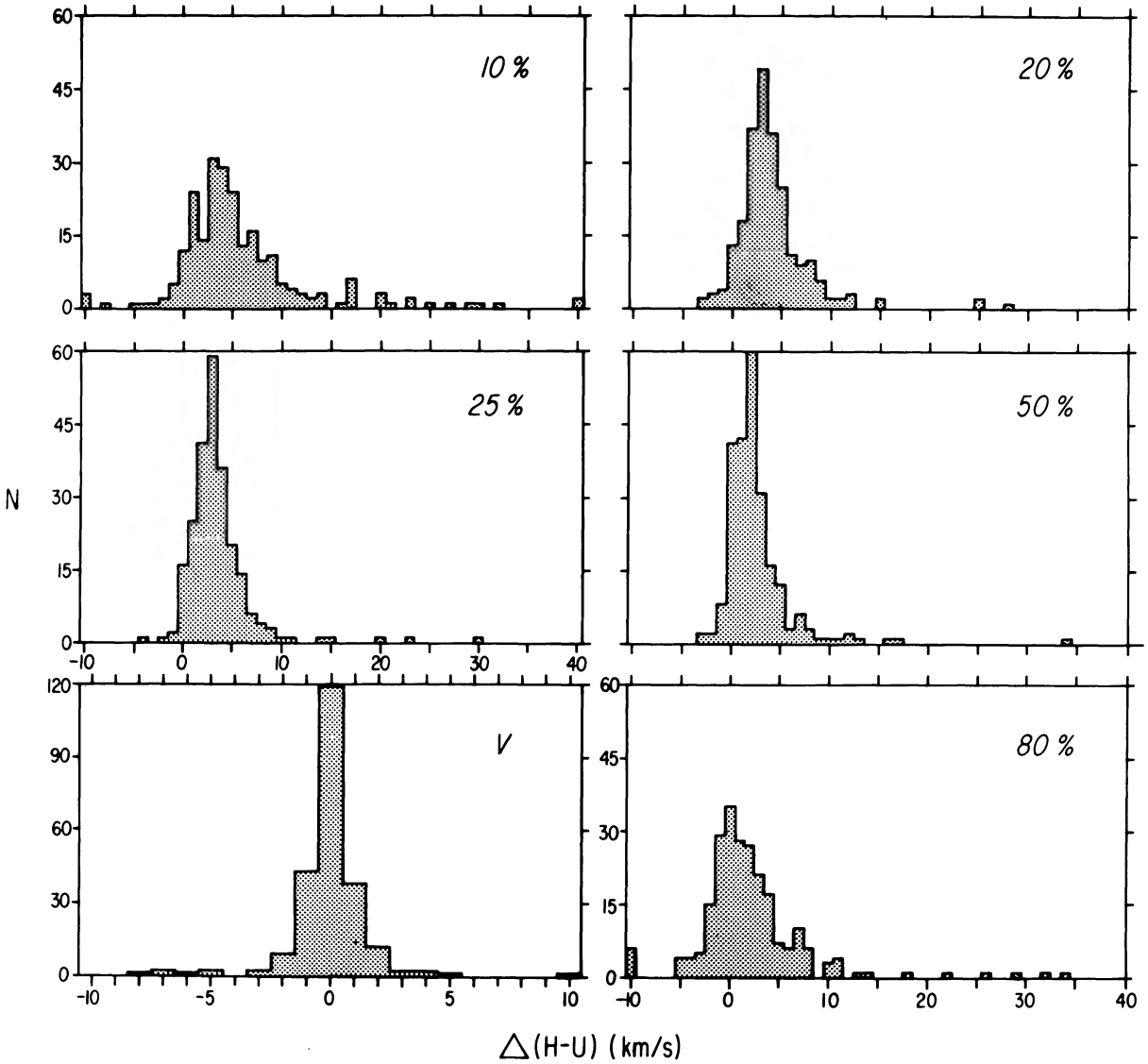

FIG. 4.—Histograms of the differences between Hanned and unsmoothed data at 10%, 20%, 25%, 50%, ad 80% levels, and for the systemic velocity estimates. All abscissae in units of km s^{-1}.

There is one (+26) outlier from 50% and two (−34, +22) km s^{-1} outliers from the 20% levels. Both comparisons are a factor of 2 worse if they are made without regard to the GS signal-to-noise ratio. We conclude that reproducible widths are obtained when the signal-to-noise ratio is adequate, and the same measuring precepts are followed: achieved precision is determined largely by the signal-to-noise ratio.

The differential width diagram shown in Figure 2 may be used as a diagnostic for the reliability of the measured widths. In practice the standard two-horned profiles fall on a well-determined locus. Remaining points on the right are due to highly asymmetric profiles (UGC 5364, UGC 6583, UGC 8774, UGC 9904, and UGC 9794). Points falling to the left of the locus are invariably due to the discrete addition of extra components to the regular profiles. The UGC lists UGC 5561, UGC 9127, UGC 9595, and UGC 10202 as multiple systems with nearby companions. The profile widths of most objects falling off the locus or with 20%–50% differences larger than 40 km s^{-1} cannot be unambiguously adjusted, and so should be excluded from calibration studies.

d) Systemic Velocities of Mapped Objects

In previous papers (e.g., GS; Helou, Hoffman, and Salpeter, 1984) the H I parameters are estimated from integral profiles, which are obtained after making an allowance for the effects of sidelobes, by mapping the H I along the major axis of each galaxy. We now compare our results obtained from observations of the central positions alone with the similar results of GS on 26 galaxies in common. For 23 objects with modest systemic velocity error estimates in GS, the mean velocity difference is +1.9 ($\sigma = 4.6$) km s^{-1}; for the 15 GS objects with comparable signal-to-noise ratios ≥ 10,

$$\langle V - V_{GS} \rangle = -0.27 \pm 0.76 \ (\sigma = 2.94) \text{ km s}^{-1}.$$

TABLE 1

H I PARAMETERS OF SAMPLE

UGC	OTHER NAME	α	δ	τ	a b ('x')	m_z	$V_\odot$	ΔV_{20}	ΔV_{25}	ΔV_{50}	ΔV_{80}	asy	$\int$ SdV mJy kms^{-1}	f_H	M_H ($10^9 M_\odot$)	rms mJy	S/N
(1)	(2)	(3)	(4)	(5)	(6)	(7)	(8)	(9)	(10)	(11)	(12)	(13)	(14)	(15)	(16)	(17)	(18)
01664		20738	73741	SBb	2.6 1.4	14.7	7269	471.3	467.7	448.0	419.9	1.36	5186	1.118	0.296+2	2.59	8
02153	NGC1030	23703	174838	S?	1.7 0.7	14.5	8552	677.6	675.9	667.3	614.6	1.13	5275	1.046	0.389+2	1.16	11
02241	NGC1085	24349	32350	Sb	2.5 1.8	13.6	6789	413.5	407.5	381.6	359.6	1.11	12004	1.131	0.597+2	2.18	22
02627		31354	312300	Sc	2.0 1.7	14.9	4219	258.0	252.4	212.3	194.1	1.69	10480	1.097	0.204+2	4.36	16
02885		34949	352633	Sc	5.5 2.5	14.4	5802	581.4	578.1	556.0	530.3	1.06	17338	1.465	0.835+2	3.36	15
*02941	IC0357	40047	220127	SBb	1.3 1.0	14.3	6262	160.7	157.2	140.5	127.6	1.84	5585	1.038	0.217+2	5.61	10
03294		51825	35728	Sb	3.4 1.7	14.5	4145	402.9	398.4	375.2	352.5	1.30	11341	1.193	0.210+2	1.80	30
*03296		51843	45017	Sa/Sb	1.9 1.4	14.3	4264	348.1	343.4	318.3	296.5	1.06	7560	1.077	0.134+2	2.43	14
03390		55842	360620	SABdm	2.3 1.3	16.5	1519	221.4	217.3	203.7	183.6	1.28	15793	1.095	0.388+1	2.90	36
03468		62418	185100	Sc-Irr	1.4 0.4	17.0	2464	215.2	207.1	172.8	149.7	1.04	7049	1.028	0.474-1	3.61	13
03489		63034	210430	Sb-c	2.2 0.3	17.0	5457	501.5	496.7	476.4	455.9	1.06	12162	1.064	0.355+2	1.19	29
*03570	IC0454	64818	125855	SBa-b	1.9 1.0	14.5	3944	450.2	431.8	411.6	390.6	1.65	14584	1.063	0.215+2	2.42	25
*03578		64929	151850	SBa-b	1.7 0.8	14.1	4531	440.6	435.3	406.6	360.1	1.14	8879	1.048	0.173+2	1.76	20
03587		65058	192146	S	3.0 1.1	14.3	1263	231.4	228.0	214.0	184.1	1.14	23715	1.134	0.354+1	1.35	91
03691		70510	151533	Sc	2.4 1.1	13.4	2202	249.1	245.5	221.6	196.1	1.03	15872	1.094	0.720+1	2.69	32
03974		73903	165507	Dwrf Ir	5.0 4.0	15.4	269	69.2	66.2	50.5	34.3	1.04	21356	1.576	0.777-1	4.72	87
*04180	IC2219	75932	273440	Sc	1.5 0.6	14.5	5231	358.6	353.5	333.3	313.7	1.08	5507	1.035	0.144+2	2.66	10
04308		81430	215020	SBc	2.2 1.8	14.5	3566	266.0	260.4	243.9	229.1	1.06	11454	1.113	0.145+2	3.66	15
*04329		81607	212040	Sc	2.5 1.5	15.0	4098	243.0	238.3	219.6	197.1	1.12	7040	1.116	0.119+2	2.42	16
04660		85116	344451	Dwrf Sp	1.7 1.3	17.0	2201	69.3	67.7	57.1	44.3	1.38	5676	1.06	0.267+1	7.41	14
*04685		85417	132328	S	1.4 0.6	14.2	3982	333.7	330.2	313.9	292.9	1.03	5885	1.031	0.844+1	1.55	14
04744	NGC2735	85942	260758	... pair	1.1 0.4	14.2	2454	422.9	414.2	392.4	364.1	1.08	11598	1.019	0.627+1	1.96	19
04752	NGC2738	90107	221001	S	1.5 0.7	13.8	3104	314.6	301.5	260.6	244.0*	1.09	7753	1.037	0.685+1	2.94	12
*04781		90354	63023	Sc	1.9 0.7	14.9	1445	163.4	159.8	141.9	106.0	1.31	11870	1.055	0.191+1	4.25	22
04837		90903	354407	Dwrf Sp	2.1 1.1	15.5	1878	123.2	116.6	104.2	55.6	1.17	5981	1.076	0.207+1	2.60	26
*04968		91839	32150	Sb	1.9 0.3	15.1	3519	275.7	272.3	256.3	239.3	1.05	9199	1.048	0.101+2	5.13	9
*05010	NGC2862	92200	265935	S	2.4 0.6	13.8	4091	606.2	604.0	592.3	561.5*	1.02	11262	1.080	0.185+2	2.90	9
*05030	NGC2882	92356	81015	S	1.7 0.9	13.5	2150	306.6	303.8	284.6	267.1	1.29	3723	1.050	0.145+1	1.69	11
*05056	NGC2894	92650	75614	Sa	2.3 1.1	13.4	2146	414.0	410.3	397.5	383.5	1.21	11216	1.088	0.451+1	3.27	12
05059	IC2487	92720	201834	Sb	1.9 0.5	14.2	4336	395.9	392.5	374.3	351.4	1.00	9612	1.051	0.170+2	3.08	11
05081	NGC2906	92927	83951	Sc	1.5 0.9	13.1	2143	364.4	362.7	341.5	324.6*	1.01	4176	1.042	0.161+1	2.00	7
05095	NGC2913	93122	94215	S	1.2 0.8	14.1	3058	235.1	233.6	225.8	213.7	1.40	2719	1.029	0.222+1	2.40	9
05102	NGC2919	93207	103027	Sb-c	1.7 0.6	13.6	2428	342.0	336.5	319.7	297.6	1.55	5696	1.043	0.290+1	1.75	16
05134	NGC2939	93528	94453	Sb-c	2.6 0.9	13.5	3338	368.6	364.6	346.5	329.2	1.01	16133	1.100	0.169+2	2.58	24
05141	NGC2948	93621	71100	SBb/SBc	1.7 0.9	13.8	4983	395.8	389.2	380.7	353.9	1.43	5392	1.050	0.124+2	2.06	16
05160	NGC2958	93800	120656	SB:b-c	1.1 0.8	13.9	6663	416.1	410.1	381.3	343.7	1.02	4279	1.026	0.176+2	1.59	9
*05173		93850	113827	Sb	2.2 0.3	15.1	6238	507.4	503.4	490.7	459.1	1.33	9457	1.064	0.352+2	4.07	9
05181	NGC2966	93935	45408	SB?	2.3 0.9	14.0	2042	255.5	253.4	242.9	229.8	1.34	6580	1.081	0.233+1	3.05	15
05215		94235	92033	Sb-c	1.7 0.9	13.8	5484	427.3	415.6	403.7	377.8	1.15	9052	1.050	0.255+2	3.75	12
*05218		94252	63623	Sc	2.0 1.0	15.0	3089	194.8	192.5	181.5	159.4	1.02	12771	1.068	0.109+2	6.21	14
05220	NGC2987	94305	51025	Sa-b	1.5 0.6	13.9	3742	357.2	353.9	344.9	328.0*	1.11	5342	1.035	0.663+1	2.45	10
*05228		94329	15400	SB...	2.6 0.8	14.1	1874	287.4	278.1	261.0	243.9	1.13	16007	1.097	0.469+1	7.09	10
05229	NGC2990	94340	55623	S?	1.1 0.6	12.5	3084	316.1	309.8	284.6	258.5	1.21	12858	1.021	0.105+2	2.24	23
*05265	NGC3018	94707	05122	S	1.3 1.0	14.2	1862	173.2	168.2	111.0	45.2	1.01	13716	1.038	0.373+1	4.77	25
05266	NGC3016	94709	125544	Sb	1.2 1.0	13.7	8970	499.3	492.6	452.8	429.3	1.40	6484	1.034	0.493+2	2.68	11
05272		94726	314320	Irr	2.2 0.8	14.7	517	94.6	91.2	75.9	55.1	1.01	12424	1.073	0.274+0	6.09	28
05325	NGC3049	95210	93035	SBb	2.5 1.6	13.5	1498	215.7	210.8	199.8	186.9	1.21	10097	1.121	0.192+1	2.42	25
05326		95228	333001	Irr	1.1 0.9	14.5	1411	123.6	119.1	100.5	75.1	1.07	4040	1.028	0.736+0	2.64	16
05340		95353	290347	DWF Pec	2.6 1.1	15.2	503	99.2	95.9	74.3	36.4	1.05	18493	1.106	0.373+0	3.04	88
*05358		95606	113745	SBb	1.7 1.1	14.9	2914	216.6	214.0	201.2	184.7	1.07	4724	1.057	0.360+1	2.48	12
05360	NGC3075	95614	143938	Sc	1.2 0.8	14.5	3582	302.9	299.3	269.6	243.8	1.40	13958	1.029	0.161+2	2.54	30
05364	D69,LeoA	95629	305907	Dwrf Ir	5.5 3.5	13.6	10	66.3	63.8	41.5	34.9a	3.06	31002	1.70	0.150-1	5.55	206
05376		95751	33656	S-Irr	2.1 0.7	14.5	2050	393.4	390.6	372.0	349.2	1.23	12630	1.065	0.444+1	4.88	8
*05396		95900	105953	Sc	1.7 0.5	14.6	5399	351.9	346.2	334.2	315.5	1.11	5670	1.041	0.153+2	2.66	9
05436		100237	193145	S	1.5 0.6	14.3	3767	311.2	307.5	290.1	273.0	1.63	8644	1.035	0.113+2	2.50	16
*05452	NGC3118	100417	331627	Sb-c	2.5 0.3	14.4	1342	232.0	227.3	200.5	177.3	1.12	18150	1.083	0.314+1	3.33	30
05471	NGC3131	100552	182833	SB:b	2.3 0.7	14.0	5098	551.0	537.7	521.6	499.1	1.04	4631	1.076	0.117+2	1.07	14
05493		100844	04127	Sb/SBc	1.7 1.4	14.0	3649	262.5	256.3	231.7	197.4	1.31	5537	1.068	0.667+1	3.59	10
05512	NGC3165	101056	33725	Irr	1.6 0.8	14.5	1328	157.5	154.4	138.5	114.2	1.41	3921	1.044	0.509+0	2.67	14
*05537		101304	73444	Sc	2.5 0.2	15.1	3756	308.3	304.5	289.3	269.9	1.68	9928	1.081	0.131+2	2.91	24
05561	IC0602	101542	71801	S	0.9 0.6	13.4	3747	323.2	312.0	220.4	77.1	1.14	10235	1.015	0.126+2	2.40	22
05601	NGC3221	101935	214919	SBc-Irr	3.3 0.8	14.3	4102	570.0	562.4	537.7	441.5	1.13	25586	1.147	0.445+2	3.27	20
05633		102159	150034	Sb IV-V	2.6 1.7	15.4	1382	177.6	175.8	165.9	150.9	1.53	12012	1.133	0.202+1	2.20	51
*05642		102302	115944	Sb-c	1.7 0.2	14.8	2351	257.5	255.2	244.2	218.4	1.01	5624	1.039	0.269+1	2.41	12
05646		102312	143701	S	2.5 0.7	14.2	1370	235.6	233.1	221.9	211.6	1.10	9757	1.089	0.155+1	2.64	21

TABLE 1—*Continued*

UGC	OTHER NAME	α	δ	τ	a b ('x')	m_z	$V_\odot$	ΔV_{20}	ΔV_{25}	ΔV_{50}	ΔV_{80}	asy	$\int$ SdV mJy kms^{-1}	f_H	M_H ($10^9 M_\odot$)	rms mJy	S/N
(1)	(2)	(3)	(4)	(5)	(6)	(7)	(8)	(9)	(10)	(11)	(12)	(13)	(14)	(15)	(16)	(17)	(18)
05651		102343	174553	Sc	1.4 1.1	14.4	5568	229.0	225.7	213.1	200.6	1.13	8330	1.044	0.244+2	4.02	13
05687		102638	62300	Sc	2.1 .22	14.9	3561	279.6	276.3	264.5	236.5	1.23	11440	1.041	0.144+2	4.03	16
05711	NGC3270	102844	250735	Sb	3.1 0.8	14.1	6261	545.9	541.7	519.7	460.3	1.07	10154	1.132	0.415+2	3.78	9
05741	IC622	103204	112728	Sc	2.8 .35	14.1	1392	359.7	357.2	325.8	310.5*	1.43	4146	1.102	0.699+1	2.61	9
05764		103354	314826	Dwrf Ir	2.0 1.2	15.6	582	115.6	111.7	100.8	89.7	1.13	10713	1.075	0.317+0	2.66	48
05829		103951	344247	Dwrf Ir	5.3 4.5	15.1	636	82.5	78.7	60.9	35.1	1.11	23253	1.685	0.138+1	4.93	78
05852	NGC3356	104136	70118	Sb	1.8 0.8	13.3	6177	378.6	373.4	338.0	308.1	1.02	12477	1.052	0.449+2	4.10	13
05897		104504	112031	Sc	2.8 0.9	14.0	2718	314.8	310.7	296.5	280.0	1.28	11958	1.113	0.837+1	2.46	24
*05906	NGC3380	104527	285159	S	1.6 1.3	13.6	1606	138.5	135.6	119.8	107.3	1.28	2164	1.059	0.521+0	2.08	10
05931	NGC3395	104702	331445	S(c)	1.8 1.0	12.1	1620	224.5	211.1	176.3	125.4	1.13	19959	1.058	0.504+1	3.36	35
05965		104841	141553	SBb-c	1.7 0.1	14.9	3073	275.7	272.4	256.3	241.3	1.37	14524	1.038	0.124+2	6.26	12
*05980	NGC3434	104923	40326	Sb	2.3 1.9	13.4	3641	291.4	282.3	252.2	234.7	1.28	15078	1.125	0.193+2	3.14	25
05989		104951	200326	Irr	1.5 0.5	14.2	1126	164.3	159.4	142.2	121.3	1.2	7779	1.03	0.809+0	3.136	10
*05994		104956	101700	Sc	1.7 0.1	15.6	6389	355.1	352.6	343.8	333.4	1.06	5811	1.038	0.222+2	2.84	10
06007	NGC3447B	105049	170305	Irr	1.7 0.8	14.3	1096	122.8	115.3	85.2	55.6	1.26	15781	1.048	0.152+1	2.36	77
06104		105912	165233	Sb-c	1.5 0.4	14.4	2947	261.9	258.0	240.7	205.2	1.15	7067	1.032	0.556+1	1.52	24
*06200		110651	01023	Sa	2.0 0.8	14.5	3859	360.5	357.2	325.6	304.4	1.74	15917	1.062	0.217+2	3.36	28
*06296		111413	180427	S	1.3 0.4	14.3	979	209.5	204.8	182.2	154.7	1.30	1752	1.025	0.133+0	1.00	11
06327	NGC3618	111553	234430	Sb	1.0 0.8	14.4	6807	310.8	307.4	284.2	250.5	1.05	3090	1.023	0.136+2	1.43	10
06351	NGC3633	111751	35138	Sa	1.2 0.4	14.3	2598	348.4	345.7	324.5	303.3	1.13	2984	1.022	0.172+1	1.67	7
06376	NGC3646	111905	202643	Sc	3.8 2.2	11.5	4249	540.3	536.6	511.3	475.3	1.13	19909	1.260	0.411+2	2.79	20
*06449		112358	114300	SBb-c	1.7 0.8	15.2	3205	238.2	235.0	221.8	208.9	1.09	8075	1.048	0.761+1	4.31	11
06464	NGC3691	112532	171146	Pec	1.1 0.9	13.1	1080	149.7	146.7	128.1	80.9	1.11	3116	1.028	0.295+0	2.00	13
06469		112543	25548	S...	0.9 .35	14.1	6841	379.0	374.0	346.9	321.7*	1.57	4183	1.013	0.179+2	2.99	16
06476		112558	234050	Sb	1.5 1.1	14.4	7328	322.0	318.5	300.1	279.9	1.12	3798	1.048	0.198+2	1.78	12
06479	NGC3697	112613	210416	Sb/SBb	2.5 0.7	14.1	6263	530.2	527.8	517.5	498.7	1.04	12088	1.089	0.475+2	3.74	11
06493	NGC3701	112651	242210	Sb-c	2.0 0.9	14.1	2805	273.6	270.2	257.4	242.7	1.06	18190	1.065	0.138+2	2.31	42
06583	Mark181	113418	201450	..PECpr	0.7 0.3	13.9	6208	377.6	372.4	308.0	287.7	1.23	4749	1.008	0.170+2	1.57	11
06586		113426	155050	Sb/Sbc	2.2 1.0	14.5	3959	289.3	281.9	257.0	237.4	1.14	11496	1.079	0.175+2	2.70	21
06621	NGC3786	113704	321108	Sa	2.2 1.1	13.0	2725	400.7	377.4	331.2	243.0*	1.44	4908	1.082	0.368+1	2.31	11
06623	NGC3788	113706	321235	S...	1.8 0.6	13.2	2687	562.1	557.0	501.3	476.6*	1.01	9359	1.048	0.660+1	3.59	7
06630	NGC3799	113733	153617	S	0.7 0.5	14.4	3312	442.0	440.0	425.1	409.7*	1.29	3689	1.010	0.364+1	0.64	20
06634	NGC3800	113737	153711	S	1.9 0.5	13.1	3302	446.3	442.5	416.1	389.3*	1.03	4701	1.051	0.479+1	1.26	11
06654	NGC3815	113903	250438	Sa-b	1.9 1.0	14.2	3711	378.2	363.3	338.6	303.1	1.20	7192	1.063	0.967+1	1.20	9
*06666		113945	161721	S	1.1 0.4	14.3	3087	209.6	206.8	193.8	175.0*	1.40	2634	1.019	0.227+1	2.38	7
06693	NGC3832	114055	230010	SBc	2.2 1.8	14.0	6910	193.8	190.2	170.1	147.9	1.33	8505	1.113	0.420+2	2.88	22
06722	NGC3863	114231	84441	Sb-c	2.8 0.6	14.0	4492	512.6	507.5	492.4	475.2	1.08	13331	1.106	0.266+2	2.80	17
*06730		114252	92623	S(a-b)	1.1 0.8	13.4	2894	178.0	171.1	147.9	103.9	1.68	4104	1.026	0.306+1	2.75	12
06790	NGC3902	114643	262403	SBb/Sc	1.7 1.3	14.0	3601	260.7	256.7	239.1	220.3	1.14	8766	1.064	0.112+2	3.11	16
06801	NGC3912	114729	264528	S-Irr	1.8 1.0	13.2	1789	253.3	243.4	173.8	83.5	1.15	5647	1.058	0.173+1	2.29	16
06872	IC2973	115115	333835	SBc	1.5 0.8	14.5	3205	215.8	212.4	182.6	151.1	1.07	6322	1.040	0.636+1	2.79	14
06886		115237	62646	SBb	1.3 0.9	14.5	6980	365.6	363.5	352.1	336.3	1.08	5547	1.035	0.254+2	4.19	7
06898	IC0746	115300	261000	S	1.3 0.3	14.5	5027	309.2	284.5	270.8	244.5	1.42	7430	1.024	0.179+2	3.05	13
06967	NGC4017	115611	274357	Sb/SBc	1.8 1.5	13.5	3456	300.8	295.7	260.8	235.1	1.29	16818	1.077	0.201+2	4.02	21
07012		115929	300740	Sc	2.1 1.1	14.3	3081	218.8	214.5	196.3	181.4	1.04	10041	1.076	0.958+1	5.07	14
07021	NGC4045	120008	21526	Sa	3.0 2.0	13.5	1978	327.1	324.1	300.1	285.1	1.06	9482	1.179	0.357+1	3.04	12
07048	NGC4067	120138	110800	Sb	1.2 0.9	13.2	2426	272.7	268.8	244.1	199.0	1.17	3883	1.031	0.204+1	1.77	12
07130	NGC4134	120638	292720	Sb	2.3 0.8	13.8	3825	351.5	346.7	328.5	315.8	1.33	14662	1.079	0.217+2	2.85	20
07193	NGC4162	120919	242405	Sc	2.5 1.4	12.6	2572	333.5	331.1	319.2	300.8	1.12	10626	1.112	0.716+1	3.13	17
07211	NGC4175	120959	292650	S...	2.1 0.4	14.2	3924	242.5	239.4	205.7	203.5	1.01	2825	1.060	0.432+1	2.33	8
07225	NGC4185	121050	284722	Sb	2.9 2.2	13.5	3903	391.7	383.8	367.0	354.4	1.28	8494	1.184	0.143+2	4.06	10
07321		121502	224901	Sc	5.5 0.3	14.0	418	224.4	220.7	207.2	190.2	1.27	25223	1.343	0.454+0	2.33	60
07333	IC3115	121526	65553	SBc	1.7 1.3	14.4	2332	132.4	128.1	117.4	105.0	1.36	7966	1.044	0.391+1	4.31	20
07354	Mark49	121636	40801	...	0.5 0.4	14.5	1528	72.8	63.2	49.0	31.4	1.33	2070	1.006	0.388+0	2.15	19
07547		122418	115011	Dwrf Ir	1.6 1.1	15.5	1100	82.8	79.6	66.6	48.9	1.12	13981	1.052	0.143+1	4.02	54
07663	NGC4495	122854	292446	Sa-b	1.6 0.9	14.1	4549	389.4	385.4	367.0	352.4*	1.16	12373	1.046	0.252+2	5.78	10
07932		124307	133512	SB ..pr	1.6 0.8	14.6	968	174.6	172.6	164.4	146.0	1.48	3710	1.044	0.299+0	2.91	10
08020	NGC4771	125048	13230	Sc	4.0 0.9	13.3	1135	291.6	287.5	276.6	263.5	1.01	9909	1.209	0.119+1	4.71	11
08021	NGC4772	125056	22627	Sa	2.9 1.4	12.9	1043	467.2	456.3	436.8	397.7	1.37	8908	1.139	0.843+0	2.85	10
08091	DDO155	125610	142913	Irr	1.1 0.9	15.3	213	41.4	38.7	27.4	16.2	1.65	7765	1.028	0.197-1	5.06	55
08121	NGC4904	125825	01435	SBc	2.4 1.5	13.2	1174	210.1	206.4	187.0	159.3	1.04	10766	1.110	0.128+1	6.00	11
08255		130827	114433	Sc	1.7 1.2	14.4	3366	211.1	209.7	190.2	171.1	1.20	8736	1.060	0.958+1	2.77	20
08262		130852	00056	S	1.3 0.7	14.3	3839	343.5	341.3	330.0	319.3	1.39	3902	1.030	0.530+1	4.22	7
08271	NGC5014	130913	363257	S...	1.7 0.6	13.5	1151	215.6	208.3	163.2	141.8*	1.04	6341	1.044	0.967+1	6.37	10
08410	NGC5116	132034	271430	Sc	2.3 0.7	13.7	2885	364.7	358.5	340.0	322.9	1.10	6834	1.076	0.586+1	2.51	11

TABLE 1—*Continued*

UGC	OTHER NAME	α	δ	τ	a b ('x')	m_z	$V_\odot$	ΔV_{20}	ΔV_{25}	ΔV_{50}	ΔV_{80}	asy	$\int$ SdV mJy kms^{-1}	f_H	M_H ($10^9 M_\odot$)	rms mJy	S/N
(1)	(2)	(3)	(4)	(5)	(6)	(7)	(8)	(9)	(10)	(11)	(12)	(13)	(14)	(15)	(16)	(17)	(18)
08411	NGC5117	132035	283443	SBc?	2.3 0.7	13.7	2392	235.8	233.6	223.1	203.5	1.13	9128	1.076	0.543+1	4.30	11
08475	NGC5174	132657	111553	Sc	3.7 2.0	13.7	6840	610.4	606.1	588.6	562.9	1.17	14597	1.237	0.788+2	3.47	14
08507		132834	194140	(Irr)	1.6 0.9	14.0	997	107.9	100.8	81.0	47.0	1.17	3998	1.046	0.388+0	3.11	17
08516		132928	201523	Sc	1.1 0.8	13.8	1025	124.0	119.5	100.6	63.7	1.26	3887	1.026	0.393+0	2.50	17
08573	NGC5230	133305	135548	Sc	2.1 1.8	13.4	6858	174.2	168.0	151.6	135.3	1.29	10351	1.107	0.505+2	2.79	32
08645	NGC5258	133725	10510	S	1.7 1.4	13.8	6781	503.6	488.0	438.4	354.8	1.05	8977	1.068	0.407+2	2.44	10
08693		134216	352637	S	1.3 0.4	14.5	2438	261.3	251.1	243.4	227.7*	1.24	7797	1.025	0.474+1	5.61	9
*08728		134543	73840	SB...	1.5 0.8	14.9	6963	336.5	333.8	332.9	315.7*	1.20	5873	1.040	0.276+2	2.64	16
*08774	NGC5331	134943	22048	DBL SYS	1.1 0.8	14.3	9904	544.3	514.5	434.0	364.5	1.05	4722	1.026	0.443+2	1.85	7
08831	NGC5356	135228	53445	Sb	3.0 0.8	14.1	1370	292.7	288.7	275.5	260.6	1.25	4237	1.125	0.789+0	1.56	15
08853	NGC5364	135341	51533	Sb/Sc	7.2 5.5	13.2	1242	298.5	294.6	276.5	260.1	1.29	23591	2.155	0.688+1	4.88	28
08865	NGC5375	135440	292426	SBb	3.5 2.7	13.2	2387	307.6	295.3	284.6	268.6	1.61	10470	1.272	0.749+1	7.24	10
*08896		135609	72733	S	1.5 0.2	15.0	4401	303.7	300.4	289.7	274.4	1.23	5871	1.030	0.109+2	2.05	12
08918		135746	91230	S	1.7 0.3	14.8	4100	327.2	322.4	305.5	285.3	1.37	6603	1.040	0.108+2	1.52	22
08948		140004	91910	SBb	1.5 0.7	15.0	6011	386.4	381.3	339.8	296.2	1.07	7037	1.037	0.247+2	2.73	11
*08963	NGC5440	140050	345945	Sa	3.2 1.6	13.4	3689	624.6	624.0	610.4	594.5*	1.17	9516	1.171	0.149+2	2.59	11
08996		140218	143107	Sc	1.7 0.2	15.5	7185	442.1	431.2	417.5	400.0	1.16	6064	1.039	0.307+2	2.19	10
*09007		140238	93441	S dm	1.0 0.8	15.6	4619	55.4	52.0	39.6	18.7	1.23	1429	1.023	0.481+1	1.86	19
09020	NGC5470	140402	61601	Sb	2.6 0.4	14.5	1026	264.5	261.7	250.5	230.8	1.00	5625	1.090	0.570+0	2.23	13
09062	IC0984	140746	183551	Sb	1.9 0.4	14.5	5110	417.0	414.5	403.2	387.4	1.33	3313	1.050	0.864+1	1.98	7
09065	NGC5492	140814	195046	S	1.8 0.4	13.7	2269	373.4	368.4	355.6	334.7	1.08	10138	1.045	0.526+1	2.79	15
*09072	NGC5491	140828	63601	S	1.6 1.0	13.9	5890	498.4	494.5	467.4	425.6	1.59	6144	1.049	0.209+2	2.18	12
*09113		141206	353917	S	2.3 0.6	15.7	3188	290.3	288.9	281.6	244.9	2.16	9860	1.074	0.107+2	7.08	9
09116	NGC5522	141226	152245	Sb	1.8 0.3	14.1	4573	456.2	452.0	435.4	379.0	1.06	6684	1.045	0.138+2	1.44	14
*09121		141248	155834	Sb-c	1.6 0.7	14.8	5322	369.3	366.1	352.1	336.3	1.07	5406	1.041	0.151+2	1.35	17
09127	NGC5529	141327	362730	Sc	6.2 0.7	12.9	2882	603.4	600.4	570.1	477.8	1.16	26831	1.428	0.320+2	4.38	14
09133	NGC5533	141400	353433	Sb	3.7 2.0	13.0	3867	464.3	462.1	451.2	431.2	1.24	8269	1.237	0.151+2	3.52	10
*09138		141429	231347	Sc	1.9 0.2	15.5	4601	330.1	327.2	310.3	296.1	1.18	7131	1.048	0.152+2	2.73	11
09172	NGC5560	141734	41318	SBb	4.0 0.9	13.7	1718	276.3	270.8	227.7	179.1	1.07	5465	1.209	0.178+1	2.48	11
09176		141801	41242	Sc	2.0 1.6	14.9	1771	108.0	104.3	87.3	59.8	1.25	7777	1.092	0.243+1	4.06	23
*09180		141820	352453	Sc	1.9 1.3	14.7	3602	203.0	201.0	192.0	167.2*	1.35	6027	1.073	0.833+1	7.28	8
09187	NGC5577	141842	33950	Sb	3.2 0.9	13.6	1489	255.2	252.9	242.4	229.8	1.09	10225	1.142	0.234+1	7.10	8
*09215		142054	15701	SBc	2.5 1.3	13.6	1387	235.8	233.1	221.6	189.2	1.14	19543	1.108	0.373+1	6.62	16
*09253		142449	314426	Sb-c	1.8 0.4	14.7	3927	303.7	298.3	275.6	255.6	1.10	4940	1.045	0.784+1	2.16	13
09255	NGC5619	142447	50135	Sb	2.4 1.1	14.0	8388	747.1	743.8	716.2	683.5	1.25	3513	1.094	0.254+2	1.12	11
*09299		142702	01221	Sc	1.7 0.9	14.7	1552	197.7	191.8	167.8	126.3	1.23	25063	1.050	0.570+1	8.80	19
09300	NGC5641	142705	290240	SBb	2.6 1.4	13.6	4345	536.4	534.3	524.8	514.9	1.48	6258	1.118	0.129+2	2.73	8
09334	NGC5652	142831	61158	Sb	2.1 1.5	13.8	7496	431.2	428.8	417.0	396.9	1.07	23415	1.092	0.135+3	6.69	13
09335	NGC5657	142833	292400	SB:b	1.9 0.7	14.4	3906	351.5	348.8	334.9	318.9	1.23	8290	1.055	0.131+2	2.01	19
*09341	IC1024	142855	31348	S0?	1.6 0.6	14.0	1455	246.2	228.4	195.8	126.7	1.04	7436	1.039	0.149+1	3.66	11
*09342		142851	253433	Sb	1.7 0.5	15.0	4493	367.6	365.5	349.4	342.1*	1.39	3212	1.041	0.656+1	1.72	11
*09346	NGC5661	142928	62818	SBb	1.6 0.6	14.2	2354	291.0	286.2	263.4	206.8	1.20	15947	1.039	0.860+1	1.78	40
*09348		142955	03053	S	1.8 0.3	14.6	1672	220.3	215.4	202.2	180.3	1.25	3957	1.044	0.105+1	3.04	8
09356		143028	114851	S	1.6 0.8	14.3	2225	254.3	250.6	232.3	222.6	1.15	14168	1.044	0.698+1	4.51	19
09380		143207	42847	Dwrf Ir	2.1 1.1	15.3	1685	113.1	109.1	95.5	74.5	1.09	6522	1.076	0.185+1	5.29	14
*09389		143308	130723	SBb	2.2 0.6	14.6	1823	248.8	245.1	231.3	218.2	1.00	14811	1.069	0.507+1	3.35	21
*09394		143318	132313	Sc	2.3 0.6	14.9	1800	198.5	196.0	183.2	154.4	1.13	6433	1.074	0.216+1	3.72	10
*09414		143500	182753	Sc	1.6 0.2	15.6	5833	339.0	335.2	321.6	300.6	1.05	5487	1.034	0.185+2	1.71	15
09435	NGC5709	143642	303930	SBa	1.6 0.5	14.5	3708	359.2	356.0	346.1	334.0	1.14	5974	1.037	0.842+1	1.80	16
09481	NGC5735	144023	285615	SBb	2.8 2.0	13.8	3741	247.2	244.2	231.9	216.0	1.16	12244	1.164	0.197+2	2.59	31
09535	NGC5762	144619	123950	S	2.0 1.5	14.3	1792	192.5	190.4	182.4	170.8	1.05	8618	1.087	0.293+1	2.31	32
09573	IC1066	145031	32958	S	1.4 0.8	14.2	1576	222.5	218.7	203.8	181.5	1.11	8445	1.036	0.204+1	2.01	28
09574	IC1067	145034	33206	SBb	2.2 1.7	13.6	1578	224.4	222.6	213.7	199.0	1.05	7120	1.108	0.184+1	2.22	21
09595	IC1076	145241	181425	...pr	1.2 0.7	13.9	6075	338.0	333.6	312.1	290.8*	1.10	7059	1.027	0.257+2	2.57	10
09628	NGC5798	145531	301005	Irr	1.4 0.9	13.5	1791	209.7	206.0	189.3	160.6	1.16	6528	1.038	0.229+1	1.75	22
*09712		150421	124510	Sc	1.5 0.3	15.2	6857	340.8	336.8	313.6	245.3	1.19	5868	1.031	0.272+2	3.15	8
09715	NGC5850	150435	14417	SBb	5.0 4.5	13.6	2558	215.4	212.6	199.8	185.7	1.30	8508	1.644	0.865+1	2.69	24
09728	NGC5859	150519	194625	SBb	2.9 0.7	13.1	4761	476.0	470.8	452.1	433.1	1.00	9314	1.115	0.229+2	2.01	16
*09763		150948	212900	S?	2.0 0.4	15.6	4700	422.1	410.3	360.2	312.3	1.08	6973	1.055	0.159+2	1.03	20
*09772		151116	342003	SBc	1.0 0.7	16.5	2319	113.3	110.5	95.8	77.6	1.49	7589	1.021	0.437+1	4.29	23
09794		151347	104133	SBc-Irr	3.0 0.8	14.3	6446	689.1	668.9	544.9	463.8	1.05	21772	1.125	0.974+2	2.61	20
*09888	IC1125	153030	-12740	S-Irr	1.7 1.0	14.5	2796	233.4	230.5	215.7	194.8	1.13	11278	1.053	0.891+1	5.55	13
*09901		153205	122603	Sb-c	1.7 0.3	15.2	3162	241.1	237.7	223.2	210.3	1.12	5787	1.039	0.591+1	2.86	12
09904	NGC5954	153216	152210	S(c)	1.1 0.5	13.7	1960	278.5	258.9	145.7	74.0	1.18	7328	1.020	0.293+1	0.95	50
*09919		153318	124620	Sc	1.6 0.1	15.1	3185	267.9	265.0	253.1	234.7	1.09	4251	1.034	0.439+1	2.56	10

TABLE 1—*Continued*

UGC	OTHER NAME	α	δ	τ	a b ('x')	m_z	V_o	ΔV_{20}	ΔV_{25}	ΔV_{50}	ΔV_{80}	asy	$\int SdV$ mJy kms^{-1}	f_H	M_H ($10^9 M_\odot$)	rms mJy	S/N
(1)	(2)	(3)	(4)	(5)	(6)	(7)	(8)	(9)	(10)	(11)	(12)	(13)	(14)	(15)	(16)	(17)	(18)
*09920		153316	305800	Sb	1.4 0.1	15.1	9438	511.6	507.1	481.8	460.9	1.14	2906	1.026	0.258+2	1.33	10
09925		153414	163615	Sc	1.4 0.6	15.4	1913	195.4	191.8	181.8	161.2	1.30	1920	1.031	0.746+0	1.58	9
09935	NGC5964	153508	60816	SBc	4.4 3.4	14.2	1447	199.2	196.8	184.8	161.2	1.24	21420	1.432	0.645+1	1.05	136
*09951		153701	153243	Sc	1.4 0.8	15.7	2004	154.7	151.9	139.1	126.3	1.05	3827	1.036	0.163+1	1.49	26
09965	IC1132	153754	205030	Sc	1.3 1.1	14.4	4528	114.8	107.1	87.6	68.4	1.01	5374	1.041	0.113+2	1.76	34
09979		153946	03811	Dwrf Ir	1.5 0.5	15.7	1961	133.8	131.9	118.2	80.1	1.18	5436	1.034	0.210+1	6.10	8
09987	NGC5984	154033	142325	SBc	2.9 0.6	13.5	1105	243.0	239.1	226.2	209.2	1.11	12697	1.113	0.188+1	3.82	16
09991		154105	143530	Sc	1.7 0.5	15.1	1933	227.2	223.3	209.1	179.4	1.16	6579	1.042	0.263+1	1.48	28
10014		154323	123954	Dwarf	1.3 1.1	15.7	1122	121.3	117.0	102.3	88.3	1.15	11448	1.041	0.162+1	3.09	37
*10021		154335	281433	S	1.4 0.3	14.9	2145	309.5	305.6	291.0	278.7	1.21	6407	1.028	0.322+1	1.87	15
10024	NGC5990	154345	23411	Sa	1.6 0.9	13.1	3824	406.3	405.3	400.4	370.7*	1.67	2631	1.046	0.388+1	2.17	7
*10042		154631	72227	Sc	1.6 0.3	14.8	4226	348.5	346.6	337.1	320.3	1.02	4712	1.035	0.845+1	2.47	9
*10043		154630	220142	Sb/Sc	2.4 0.3	15.4	2154	341.3	337.6	321.6	307.3	1.39	17315	1.076	0.904+1	2.44	40
*10044		154642	181523	Sc	1.3 0.1	16.0	3316	219.6	217.5	197.2	177.6	1.05	2961	1.023	0.334+1	1.55	15
10079	NGC6007	155102	120627	Sc	1.7 1.2	14.1	10544	424.5	419.5	395.7	369.7	1.02	9741	1.060	0.110+3	2.55	14
10083	NGC6012	155154	144455	SBa	2.1 1.6	13.1	1855	178.6	175.9	163.7	152.9	1.08	12425	1.097	0.487+1	1.75	59
10108	IC1149	155547	121246	Sb-c	1.3 1.1	14.1	4685	208.1	200.1	185.0	174.2	1.03	4635	1.041	0.104+2	2.19	15
10113	IC1151	155616	173503	SBc	2.5 0.7	13.4	2169	252.4	248.2	234.0	213.4	1.05	9202	1.089	0.489+1	2.37	20
10127		155813	205925	Sb	1.4 0.8	14.2	4823	412.3	407.6	387.2	358.5	1.16	10751	1.036	0.257+2	1.79	20
*10130		155855	85827	Sa	1.4 0.8	15.1	5027	339.6	335.8	317.4	299.8	1.12	4156	1.036	0.106+2	1.69	15
10133	IC1158	155902	15045	Sc/SBc	2.8 1.7	14.4	1928	250.5	248.0	237.7	222.9	1.06	8879	1.147	0.375+1	2.74	18
10182	NGC6052	160301	204038	DBL SYS	0.8 0.6	14.1	4746	444.4	429.9	355.1	301.9	1.21	6359	1.013	0.144+2	1.52	13
10202	NGC6062	160410	195445	SBb	1.1 0.9	14.4	11713	412.2	406.0	325.0	197.2	1.15	8853	1.028	0.120+3	2.65	12
10235	NGC6073	160755	164941	Sc	1.2 0.6	14.5	4649	322.9	320.6	319.9	306.6*	1.17	5077	1.025	0.111+2	3.26	8
10339		161737	362400	...	0.7 .45	14.3	5046	218.3	211.5	172.2	109.0	1.08	2956	1.016	0.723+1	9.19	8
10445		163148	290519	Sc	2.9 1.9	14.2	963	155.1	150.5	128.8	110.4	1.01	15500	1.165	0.219+1	2.81	44
10521	NGC6207	164118	365532	S	3.3 1.2	11.9	850	245.8	239.2	222.4	200.9	1.02	22536	1.161	0.270+1	7.52	16
10606	NGC6255	165300	363455	SBc	3.5 1.4	13.8	923	201.9	194.6	165.2	123.4	1.54	20635	1.186	0.292+1	7.69	21
10628	NGC6267	165602	230337	SBc	1.4 1.1	14.0	2980	258.6	255.3	239.9	216.3	1.10	5993	1.044	0.586+1	2.25	17
*10721		170623	253451	Sc?	1.1 0.6	14.2	2918	285.9	282.2	267.1	250.2	1.09	6096	1.021	0.566+1	1.47	21
10747	NGC6308	170954	232623	Sc/SBc	1.3 1.0	14.4	8820	330.0	324.2	298.7	275.8	1.06	3703	1.038	0.294+2	1.59	12
11121	NGC6555	180536	173550	Sc	2.1 1.8	12.7	2222	226.4	222.3	208.1	189.7	1.00	10389	1.107	0.636+1	3.39	17
11308	NGC6674	183631	251955	SBb	4.5 2.1	13.7	3428	463.8	460.9	448.0	433.7	1.08	23738	1.321	0.397+2	1.63	52
*11708	NGC7046	211224	23738	SB	1.8 1.5	14.2	4161	302.1	296.3	282.6	255.9	1.02	8391	1.077	0.163+2	4.90	9
11786	NGC7102	213715	60333	SBb	1.7 0.9	14.4	4843	199.2	186.4	162.4	133.5	1.26	8202	1.050	0.209+2	2.63	22
11820		214704	135948	Dwrf Sp	1.5 1.0	17.0	1106	127.5	124.7	111.2	96.2	1.02	17364	1.045	0.313+1	3.30	53
11944		220936	173924	Dwrf Ir	2.3 0.8	16.0	1736	163.3	160.8	142.2	127.4	1.07	11242	1.079	0.452+1	4.87	18
12080	NGC7311	223135	51846	Sa-B	1.8 0.9	13.4	4524	519.9	514.9	497.6	478.4*	1.15	3589	1.055	0.800+1	2.55	7
12082		223153	323600	Dwrf Sp	3.5 3.0	15.6	804	80.4	77.4	66.7	51.3	1.22	16439	1.299	0.236+1	2.24	118
12212		224808	285224	Dwrf Sp	2.5 1.8	16.0	894	109.9	107.4	97.7	86.6	1.01	12246	1.131	0.176+1	1.74	76
12262	NGC7428	225445	-11856	SBa	2.5 1.3	13.8	3077	338.1	334.8	313.2	296.6	1.10	2711	1.108	0.302+1	2.05	7
12353	NGC7483	230315	31630	SBa	1.6 0.9	14.3	4939	277.3	263.2	239.1	204.0	1.83	6739	1.046	0.175+2	4.04	12
12613	D216,Peg	232604	142800	Dwrf Ir	5.0 3.0	15.5	-182	36.8	33.8	21.8	13.7a	3.14	6614	1.46	0.657-4	1.55	204
12622	NGC7682	232630	31528	SBa	1.1 0.9	14.3	5116	211.8	208.0	195.5	176.3	1.72	1191	1.028	0.324+1	1.28	9
12682		233222	175700	Irr	1.6 1.3	14.7	1388	98.5	93.3	70.5	37.8	1.02	8337	1.059	0.216+1	1.60	74
12699	NGC7714	233340	15246	S	1.8 1.3	13.1	2804	229.2	220.2	165.6	92.8	1.06	13617	1.068	0.121+2	3.83	22
12791		234617	255626	Dwrf Ir	1.7 0.6	15.2	788	112.5	108.3	91.8	67.6	1.35	8033	1.044	0.833+0	2.11	53
*12931		92448	40859	S(a-b)	0.9 0.5	14.5	5329	281.9	272.5	246.7	230.1*	1.13	3066	1.00	0.763+1	2.23	9

NOTE.—All velocities in km s^{-1}. In col. (12) an asterisk following an entry indicates that an internal peak has been removed while measuring widths; an "a" following an entry indicates a Local Group member with a distance assigned by de Vaucouleurs 1975. As explained in the text, an asterisk preceding a UGC number indicates a new systemic velocity.

Monte Carlo simulations of the effects of noise on the measuring algorithms show that at a signal-to-noise ratio of 10, σ for a single observer is 1.5 km s^{-1}. Including effects from baseline fitting and pointing errors, a realistic error estimate is $\sigma \sim 2.0$ km s^{-1}, in close agreement with the results of the above comparison. These also show that precision is not lost by observing the central profile alone, although an adequate signal-to-noise ratio is required if velocity errors are to be small.

e) Systemic Velocity Comparisons with Fisher and Tully

The largest published collection of H I data is the Fisher and Tully (1981, hereafter FT) summary of their Green Bank observations. These were obtained with a wide range of achieved signal-to-noise ratios, and the velocities were derived from graphical measurements on the smoothed profiles. Rood (1982) used these data as the primary standard in his study of the errors and variances characterizing the results of other observers. He assigns a value $\sigma \sim 8$ km s^{-1} to the data set and

finds a 2.3 ± 0.15 km s^{-1} offset for it from the average defined by other 21 cm observers.

Our data confirm this offset. For 56 galaxies in common we find

$$\langle V - V_{FT} \rangle = -3.14 \pm 1.05 \text{ km s}^{-1},$$

with $\sigma \sim 7.85$ km s^{-1}. The largest residuals are -23 km s^{-1} from UGC 8507 and UGC 9309, and $+22$ km s^{-1} from UGC 7739.

TABLE 2

EFFECT OF SMOOTHING ON MEASURED WIDTHS

Percentage Level	$H-U$[a]	$S-U$[b]	$S-H$[c]
⟨10%⟩ ...	3.81 ± 0.19	9.11 ± 0.35	4.18 ± 0.17
σ	3.09	4.91	2.58
⟨20%⟩ ...	3.12 ± 0.07	7.29 ± 0.14	3.55 ± 0.05
σ	1.87	3.39	1.53
⟨25%⟩ ...	2.88 ± 0.06	6.62 ± 0.16	3.13 ± 0.05
σ	1.69	3.00	1.42
⟨50%⟩ ...	1.60 ± 0.07	3.29 ± 0.10	1.25 ± 0.03
σ	1.58	2.53	1.09
⟨80%⟩ ...	0.88 ± 0.13	0.31 ± 0.36	-0.75 ± 0.08
σ	2.59	4.34	1.63

NOTE.—All units are km s^{-1}.

[a] Hanned minus unsmoothed differences.

[b] Hanned and boxcar smoothed minus unsmoothed differences.

[c] Smoothed minus Hanned differences.

f) Center for Astrophysics Systemic Velocities

Systemic velocity estimates from H I observations have been used for several years to test the zero point and variance of optical estimates of the systemic velocity (cf. Roberts 1972; Lewis 1975; Sandage 1978; Rood 1982; Lewis 1983*b*). Our sample, together with the companion study of Lewis (1985*a*), has 122 objects in common with CfA, which allows us to make an independent check on its characterization. A direct comparison gives excellent agreement. The largest residual is 197 km s^{-1} for UGC 9308 (NGC 5638), an elliptical galaxy that may have been detected at 21 cm, or may be contaminated by a nearby neighbor (cf. Lewis 1983*a*). If this object is deleted from the comparisons, the largest remaining residuals are -153 km s^{-1} for UGC 5471 and -114 km s^{-1} for UGC 9334.

A histogram of the 121 residuals is shown in Figure 6. These have a mean difference, after discounting differences $> 3\,\sigma$, of

$$\langle V - V_{CfA} \rangle = +1.10 \pm 3.11 \text{ km s}^{-1} \qquad (\sigma = 33.9 \text{ km s}^{-1}).$$

The mean estimated error of the CfA objects in our sample is 30.7 km s^{-1}, while the average difference is only 25.7 km s^{-1}. These values are smaller than the average error of 38 km s^{-1} found by Rood (1982). But if we follow Rood and define a dimensionless and normalized error estimate,

$$x = (V - V_{CfA})(\sigma^2 + \sigma_{CfA}^2)^{-0.5},$$

we can expect properly characterized data to give a mean $\langle x \rangle \sim 0$ and to have a σ of about unity. Our data yield $\langle x \rangle = +0.077$ ($\sigma_x \sim 1.00$) when the CfA error estimates are increased by a factor of 1.13. This is smaller than the factor of

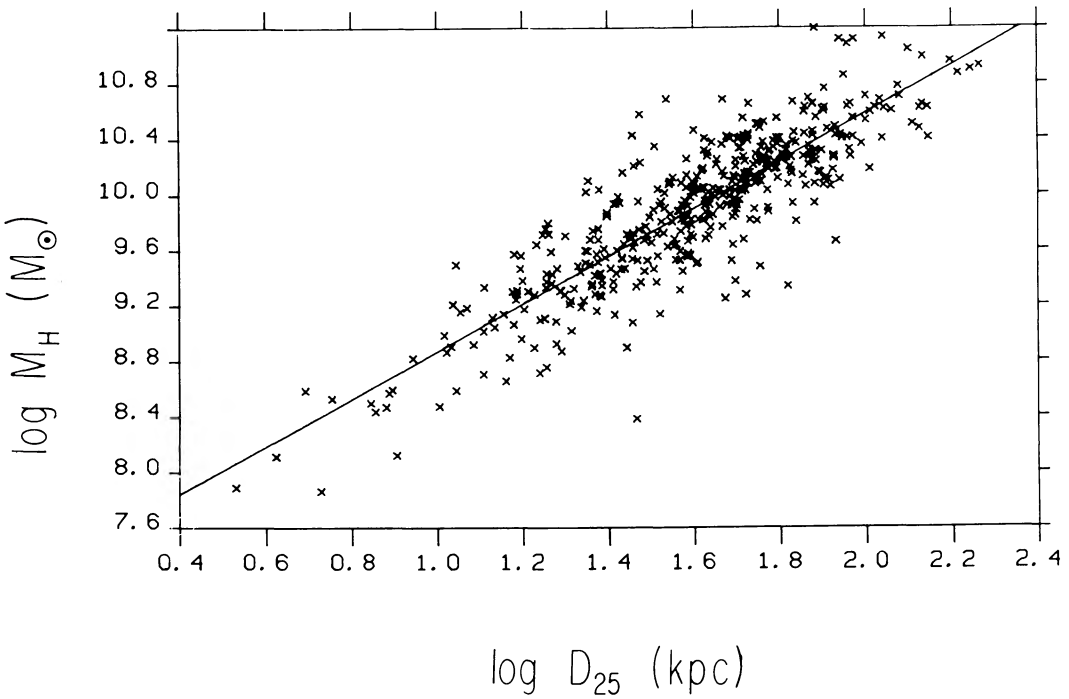

FIG. 5.—Log of the hydrogen mass in solar units after compensating for the effects of source size/(diameter at 25 mag arcsec^{-2} isophote). Distances are calculated from redshifts after a 300 sin l cos b adjustment, assuming $H = 50$ km s^{-1} Mpc^{-1}.

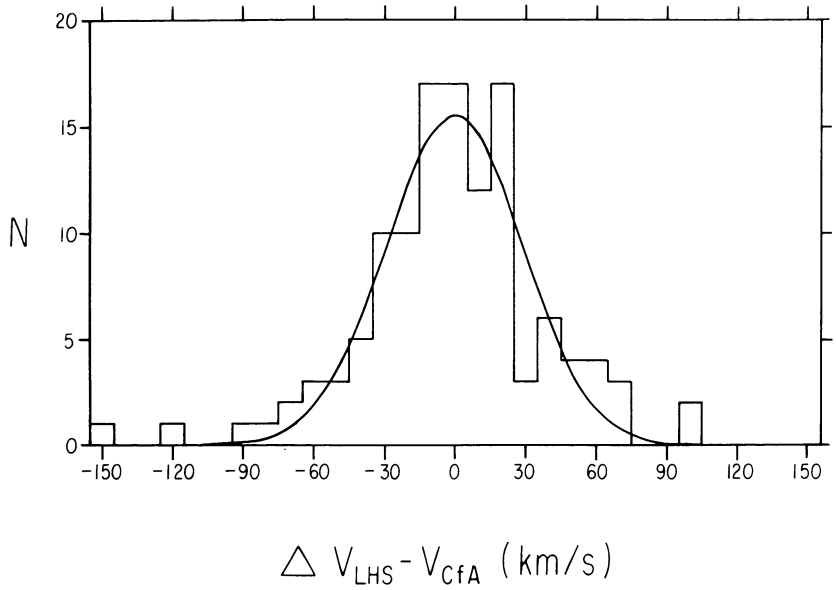

FIG. 6.—Histogram of the differences in systemic velocity $V - V_{CfA}$ between 21 cm estimates presented here and velocities of the CfA Survey (Huchra *et al.* 1983). The superposed Gaussian has a $\sigma \approx 28.7$ km s^{-1}.

1.2 suggested by Rood. We conclude that both the advertised accuracy of the CfA velocities and their estimated errors on an object-by-object basis are realistic.

Figure 6 shows a hint of a bimodal distribution of errors. Most CfA velocities are derived from measurements of absorption lines in a single spectrum; some are an average of both emission- and absorption-line velocities or an average from several spectra. A bimodal distribution is therefore expected.

IV. COMMENTS

Interference spikes occur near the profile edges of UGC 2627 and UGC 10235. These are not removed in Figure 1, and do not affect the estimated widths. By contrast, the narrow profiles of UGC 7354 and UGC 9007 are real, and show that these objects are more face-on than their axis ratios of 0.5 × 0.4 and 1.0 × 0.8 suggest.

Our signal-to-noise ratio is sufficient to show that most substantial departures from a classic two-horned spiral profile are real. The H I profiles of UGC 5561, 5601, 6583, 9794, 9904, 10182, and 11786 exhibit an additional hump on one shoulder. They all have either small companions (in the case of UGC 9904, area is mapped by Haynes 1981) or are noted in the UGC as optically asymmetric (UGC 9794 and UGC 10182 or Arp 209 [Arp 1966]). Extra components which are attributable to small companions are found within many profiles. The prototype for this behavior is UGC 10024, where the additional component is clearly separate from either of the "horns." Similar features occur in UGC 4752, 5056, 6469, 6630, 6634, 9595, and 10202. All of these objects have close companions. Some profiles have gradual shoulders, including UGC 3974, 4837, 5265, 5272, 5340, 5764, 5829, and 8271. None of the latter group has a companion or a noteworthy optical peculiarity: a gradual shoulder appears to be an intrinsic feature in these cases.

A few profiles exhibit H I absorption features. This is most marked in spectra of UGC 6476 and UGC 7663, in which Dressel and Condon (1978) detect 2380 MHz fluxes of 28 and 7 mJy. Narrow absorption-like features are also seen in UGC 6449, 9138, 9342, and 9414.

In examining our profiles, we are impressed with the number exhibiting a broad asymmetric feature that seems to be an "absorption" feature within the profile. UGC 7225 provides the prototype example of this behavior, with, in this case, horns of almost equal intensity, and a pronounced minimum on the low-velocity side. Our data set shows many instances in which the "absorbed" side has a horn with a lower intensity than its counterpart, ranging downward from UGC 7130 and UGC 6967 to UGC 3570, 5102, 5266, and 5360. Perhaps even the extreme asymmetry of UGC 5965, 6200, and 8262 is due to a more extreme incidence of the effect. Since this is not an effect that can be modeled by any perturbation of a galaxy's H I distribution without invoking absorption, we suggest that the effect is due to asymmetric H I absorption of continuum radiation within the objects, an explanation that should be confirmed by future continuum observations of the objects.

Asymmetric "absorption" is common. It is not usually due to pointing errors or to incomplete sampling of the H I. Many of the major-axis mapped profiles of GS show the same behavior, and it is seen too in the well-observed profiles of Shostak (1978), where a range of bright spirals are observed with the 11′ beam of the Green Bank 93 m telescope. The "absorption" may sometimes be almost symmetric, as the broad minima in UGC 6479, 8475, and 9920 perhaps suggest, but it is easier to notice when it occurs asymmetrically.

Departures from a regular two-horned profile noted here are generally visible in the composite spectra of GS, when they have a sufficient signal-to-noise ratio. Additional components in spectra of UGC 4752, 6634, and 9595 as well as the hump on the shoulder of UGC 6583 are seen too by Giovanardi and

Salpeter (1985), as are the broad asymmetric "absorption" feature in UGC 7255 and the narrow features of UGC 10628. The only distortion of the global profile introduced by adopting the profile observed from the center of small angular diameter galaxies with the 3'.2 Arecibo beam as the global profile is a loss of emphasis on the horns. This causes the classic shape of UGC 9987 to become almost flat-topped.

This study benefited from the generosity of J. Huchra in making available a copy of the CfA Survey in advance of publication, and from access to R. Giovanelli's list of 21-cm velocities available in 1981. This work was supported by the National Astronomy and Ionosphere Center, which is operated by Cornell University under contract with the National Science Foundation.

REFERENCES

Aaronson, M., Mould, J., Huchra, J., Schecter, P. L., and Tully, R. B. 1982, *Ap. J.*, **258**, 64.
Arp, H. C. 1966, *Ap. J. Suppl.*, **14**, 1.
Bridle, A. H., Davis, M. M., Fomalont, E. B., and Lequeux, J. 1972, *A.J.*, **77**, 405.
Davis, M., Huchra, J., Latham, D., and Tonry, J. 1982, *Ap. J.*, **253**, 423.
de Vaucouleurs, G. 1976, *Ap. J.*, **203**, 33.
_____. 1975, in *Stars and Stellar Systems*, Vol. **9**, *Galaxies and the Universe*, ed. A. Sandage, M. Sandage, and J. Kristian (Chicago: University of Chicago Press), p. 557.
Dressel, L. L., and Condon, J. J. 1976, *Ap. J. Suppl.*, **31**, 187.
_____. 1978, *Ap. J. Suppl.*, **36**, 53.
Fisher, R. J., and Tully, R. B. 1981, *Ap. J. Suppl.*, **47**, 139 (FT).
Giovanardi, C., and Salpeter, E. E. 1985, *Ap. J. Suppl.*, **58**, 623 (GS).
Gregory, S. A., and Thompson, L. A. 1978, *Ap. J.*, **222**, 784.
Gregory, S. A., and Tifft, W. 1976, *Ap. J.*, **205**, 696.
Haynes, M. P. 1981, *A.J.*, **86**, 1126.
Haynes, M. P., and Giovanelli, R. 1984, *A.J.*, **89**, 758.
Helou, G., Hoffman, G. L., and Salpeter, E. E. 1984, *Ap. J. Suppl.*, **55**, 433.
Hewitt, J. N., Haynes, M. P., and Giovanelli, R. 1983, *A.J.*, **88**, 272.
Huchra, J. 1983, in *Proc. ESO Workshop on Virgo Cluster*, ed. O. G. Richter and B. Binggeli.
Huchra, J., Davis, M., Latham, D., and Tonry, J. 1983, *Ap. J. Suppl.*, **52**, 89 (CfA).
Lewis, B. M. 1975, *Mem. R.A.S.*, **78**, 75.
_____. 1983*a*, *A.J.*, **88**, 962.
_____. 1983*b*, *A.J.*, **88**, 1695.
_____. 1985*a*, preprint.
_____. 1985*b*, *Ap. J.*, **292**, 451.
Nilson, P. 1973, *Uppsala General Catalogue of Galaxies* (*Uppsala Astr. Obs. Ann.*, Vol. **6**) (UGC).
Roberts, M. S. 1972, in *IAU Symposium 44*, *External Galaxies and Quasi-stellar Objects*, ed. D. S. Evans (Dordrecht: Reidel), p. 12.
Rood, H. J. 1982, *Ap. J. Suppl.*, **49**, 111.
Sandage, A. 1978, *A.J.*, **83**, 904.
Shostak, G. S. 1978, *Astr. Ap.*, **68**, 321.
Tammann, G. 1983, in *Proc. ESO Workshop on Virgo Cluster*, ed. O. G. Richter and B. Binggeli.
Tully, R. B. 1982, *Ap. J.*, **257**, 389.
Tully, R. B., and Fisher, R. J. 1977, *Astr. Ap.*, **54**, 661.

G. HELOU: Infrared Processing and Analysis Center, California Institute of Technology, 100-22 Pasadena, CA 91125

B. M. LEWIS: Arecibo Observatory, P.O. Box 995, Arecibo, PR 00613

E. E. SALPETER: Center for Radiophysics and Space Research, Cornell University, Ithaca, NY 14853